On the validity of foraminifera-based ENSO reconstructions

Brett Metcalfe[1,2], Bryan C. Lougheed[1,3], Claire Waelbroeck[1] and Didier M. Roche[1,2]

[1]Laboratoire des Sciences du Climat et de l'Environnement, LSCE/IPSL, CEA-CNRS-UVSQ, Université Paris-Saclay, F-91191 Gif-sur-Yvette, France
5 [2]Earth and Climate Cluster, Department of Earth Sciences, Faculty of Sciences, VU University Amsterdam, de Boelelaan 1085, 1081 HV, Amsterdam, The Netherlands
[3]Department of Earth Sciences, Uppsala University, Villavägen 16, 75236 Uppsala, Sweden

Correspondence to: Brett Metcalfe (brett.metcalfe@lsce.ipsl.fr or b.metcalfe@vu.nl)

A complete understanding of past El Niño-Southern Oscillation (ENSO) fluctuations is important for the future
10 **predictions of regional climate using climate models. Reconstructions of past ENSO dynamics use carbonate oxygen isotope ratios ($\delta^{18}O_c$) and trace metal geochemistry (Mg/Ca) recorded by planktonic foraminifera to reconstruct past spatiotemporal changes in upper ocean conditions. We investigate whether planktonic foraminifera-based proxies offer sufficient spatiotemporal continuity with which to reconstruct past ENSO dynamics. Concentrating upon the period of the instrumental record, we use the *Foraminifera as Modelled Entities* model to statistically test whether or**
15 **not $\delta^{18}O_c$ and the Temperature signal (T_c) in planktonic foraminifera directly records the ENSO cycle. Our results show that it is possible to use $\delta^{18}O_c$ from foraminifera to disentangle the ENSO signal only in certain parts of the Pacific Ocean. Furthermore, a large proportion of these areas coincide with sea-floor regions exhibiting a low sedimentation rate and/or water depth below the carbonate compensation depth, thus precluding the extraction of a temporally valid palaeoclimate signal using long-standing palaeoceanographic methods.**

20 **1.0 Introduction**

Predictions of short-term, abrupt changes in regional climate are imperative for improving the spatiotemporal precision and accuracy when forecasting future climate. Coupled ocean-atmosphere interactions (wind circulation and sea surface temperature) in the tropical Pacific, collectively known as the El Niño-Southern Oscillation (ENSO), represent global climate's largest source (Wang et al., 2017) of inter-annual climate variability (Figure 1). Due to ENSO's major socio-
25 economic impacts upon pan-Pacific nations, which, depending on the location, can include flooding, drought and fire risk, it is imperative to have an accurate understanding of both past and future behaviour of ENSO. The instrumental record of the past century provides important information (*i.e.* the Southern Oscillation Index; SOI), however, detailed observations of ENSO, such as the Tropical Oceans Global Atmosphere (TOGA; 1985-1994) experiment only provide information from the latter half of the twentieth century (Wang et al., 2017). To acquire longer records, researchers must, therefore, turn to the
30 geological record using archives such as: corals (Cole and Tudhope, 2017); foraminifera (Ford et al., 2015; Garidel-Thoron et al., 2007; Koutavas et al., 2006; Koutavas and Joanides, 2012; Koutavas and Lynch-Stieglitz, 2003; Leduc et al., 2009;

White et al., 2018); stalagmite (Asmerom et al., 2007; Zhu et al., 2017b); fish detritus (Patterson et al., 2004; Skrivanek and Hendy, 2015); lake (Anderson et al., 2005; Bennett et al., 2001; Benson et al., 2002; Conroy et al., 2008; Enzel and Wells, 1997; Higley et al., 2018; Loubere et al., 2013; Zhang et al., 2014); terrestrial (Barron et al., 2003; Barron and Anderson, 2011; Caramanica et al., 2018; Hendy et al., 2015; Staines-Urías et al., 2015); and sedimentological parameters (Moy et al.,

5   2002) including varves (Du et al., 2018; Nederbragt and Thurow, 2001, 2006) to reconstruct long-term variations in ENSO and its impact upon both regional and global sea surface temperature (SST). An integrated approach combining palaeoclimate proxies (Ford et al., 2015; Garidel-Thoron et al., 2007; Koutavas et al., 2006; Koutavas and Joanides, 2012; Koutavas and Lynch-Stieglitz, 2003; Leduc et al., 2009; White et al., 2018) and computer models (Zhu et al., 2017a) can help shed light on the triggers of past ENSO events, their magnitude and their spatiotemporal distribution. Yet, the

10 reconstruction of past ENSO using climate models has been fraught with difficulties due to the associated feedbacks of ENSO upon model boundary conditions (*e.g.*, SST, pCO_2) (Ford et al., 2015). One way to deduce the relative impact and importance of various feedbacks and, in turn, reduce model-dependent noise in our predictions, is to compare model output with proxy data (Roche et al., 2017; Zhu et al., 2017a). Such an approach, however, requires an abundance of reliable spatiotemporal proxy data from the entire Pacific Ocean. Moreover, such proxy reconstructions are subject to several

15 unknowns, uncertainties and biases, especially given that foraminiferal species preferentially flourish in a particular ecological niche. A major factor governing the spatiotemporal distribution of a given planktonic foraminiferal species is the presence of an ideal water temperature. Here, we investigate whether planktonic foraminifera-based proxies offer sufficient spatiotemporal continuity with which to reconstruct past changes of ENSO. Firstly, we investigate if planktonic foraminiferal proxies have the theoretical capacity to reconstruct ENSO dynamics (Figure 2), and secondly, if the

20 sedimentation rate (Berger, 1970a, 1971; Boltovskoy, 1994; Lougheed et al., 2018; Olson et al., 2016) or the water depth (Berger, 1967, 1970b; Boltovskoy, 1966; Lougheed et al., 2018) (and therefore potential for dissolution of carbonate sediments) in the Pacific Ocean enables the capture and preservation of the foraminiferal signal (Figure 3).

Proxies of past ENSO and Pacific SST (Ford et al., 2015; Koutavas et al., 2006; Koutavas and Joanides, 2012; Koutavas and Lynch-Stieglitz, 2003; Leduc et al., 2009; Sadekov et al., 2013; White et al., 2018) are based upon the biomineralisation of

25 the calcite, or a polymorph such as verite (Jacob et al., 2017), and shells of foraminifera (Emiliani, 1955; Evans et al., 2018; Zeebe and Wolf-Gladrow, 2001). There are three major types of foraminifera-based palaeoceanographic proxies: **(1)** those associated with the faunal composition and their abundance within deep-sea sediments that utilises either a qualitative approach (Phleger et al., 1953; Schott, 1952); a weighted average (Berger and Gardner, 1975; Jones, 1964; Lynts and Judd, 1971); a selected species approach (e.g. coiling direction, or warm-water species presence; Ericson et al., 1964; Ericson and

30 Wollin, 1968; Hutson, 1980b; Parker, 1958; Peeters et al., 2004; Ruddiman, 1971; Schott, 1966); a regression analysis (Hecht, 1973; Imbrie and Kipp, 1971; Williams and Johnson, 1975); or, a transfer function (CLIMAP Project Members, 1976; McIntyre et al., 1976; Williams, 1976; Williams and Johnson, 1975) that compares the down-core records with a dataset of 'modern' values and their associated water column parameters (Hutson, 1977, 1978). **(2)** those associated with the stable oxygen isotope composition of a whole shell analysed either individually (Feldmeijer et al., 2015; Ganssen et al.,

2011; Metcalfe et al., 2015; 2019; Pracht et al., 2018) or pooled (Garidel-Thoron et al., 2007; Koutavas et al., 2002; Stott et al., 2002, 2004), herein $\delta^{18}O_c$ (c = calcite), which can ideally be used to reconstruct SST and past oxygen isotope values in seawater $\delta^{18}O_{sw}$ (sw = seawater); and (3) those associated with the trace metal geochemistry (Stott et al., 2002, 2004), more specifically the natural logarithm of the relative concentration of Mg and Ca (ln(Mg/Ca), of the shell, based upon the temperature dependent (Elderfield and Ganssen, 2000; Nürnberg et al., 1996) incorporation and substitution of a Mg cation into the calcite lattice (Branson et al., 2013, 2016). However, the interpretation of these proxies is not straightforward, for example, $\delta^{18}O_c$ is further affected by species-specific (Feldmeijer et al., 2015; Metcalfe et al., 2015; Pracht et al., 2018) disequilibria or vital effects, which clouds the accurate reconstruction of past SST and $\delta^{18}O_{sw}$. Likewise, researchers have not been able to discount the impacts of the ambient salinity (Allen et al., 2016; Gray et al., 2018; Groeneveld et al., 2008; Kısakürek et al., 2008) and carbonate ion concentration (Allen et al., 2016; Evans et al., 2018; Zeebe and Sanyal, 2002) on the Mg/Ca content of foraminifera, nor biological effects such as growth banding (Eggins et al., 2003; Hori et al., 2018; Sadekov et al., 2008, 2009; Vetter et al., 2013).

Indeed, computation of the influence of biological and vital effects upon physiochemical proxies should be a fundamental consideration for any accurate data-model comparison. Recent attempts at circumnavigating these problems have employed isotope-enabled models (Caley et al., 2014; Roche et al., 2014; Zhu et al., 2017a) or forward-proxy models (Dolman and Laepple, 2018; Jonkers and Kučera, 2017; Roche et al., 2017) to predict potential $\delta^{18}O_c$ values in foraminifera. However, the underlying foraminiferal population can be highly sensitive to the particular parameter being tested (Mix, 1987; Mulitza et al., 1998) – culture experiments have identified temperature (Lombard et al., 2009, 2011), light (Bé et al., 1982; Bé and Spero, 1981; Lombard et al., 2010; Rink et al., 1998; Spero, 1987; Wolf-Gladrow et al., 1999) carbonate ion concentration $[CO_3^{2-}]$ (Bijma et al., 2002; Lombard et al., 2010) and ontogenetic changes (Hamilton et al., 2008; Wycech et al., 2018) as variables that drive, alter or induce changes in foraminiferal growth. Such sensitivities limit the experimental independence of a data-model comparison using the aforementioned parameters (Roche et al., 2017).

A chief parameter that has been employed in previous ENSO proxy work using individual foraminifera analysis (IFA) is the $\sigma(\delta^{18}O_c)$ parameter. This parameter $\sigma(\delta^{18}O_c)$ is used to reconstruct the downcore individual foraminifera variance in $\delta^{18}O_c$, and increased $\sigma(\delta^{18}O_c)$ is considered to correlate to increased variation in SST and, in turn, increased ENSO incidence and/or magnitude (Leduc et al., 2009; Zhu et al., 2017a) or even increased inter-annual variance in temperature. However, foraminifera are not passive recorders of environmental conditions such as SST, in that the very the ambient environment that researchers wish to reconstruct also modifies the foraminiferal population as well (Mix, 1987). Here, we use the recently developed *Foraminifera as Modelled Entities* (FAME) model (Roche et al., 2017) to take into account potential modulation of $\delta^{18}O_c$ and the Temperature recorded in the calcite, herein T_c, by foraminifera growth, an estimate of the proxy Mg/Ca. A number of models exist to determine the foraminiferal responses to present (Fraile et al., 2008, 2009; Kageyama et al., 2013; Kretschmer et al., 2017; Lombard et al., 2009, 2011; Roy et al., 2015; Waterson et al., 2016; Žarić et al., 2005, 2006), past (Fraile et al., 2009; Kretschmer et al., 2016) and future (Roy et al., 2015) climate scenarios, FAME uses the associated temperature and $\delta^{18}O_{eq}$ at each grid cell to compute a time averaged $\delta^{18}O_c$ and T_c for a given species. This model utilises the

temperature component of the Lombard *et al.* (2009) equations to simulate temperature-derived growth (Kageyama et al., 2013; Lombard et al., 2009, 2011) and subsequently growth rate-weighted $\delta^{18}O_c$ (Roche et al., 2017) and T_c for *Globigerinoides ruber*, *Globigerinoides sacculifer* and *Neogloboquadrina dutertrei*, forced by fifty-eight years of monthly ORAS S4 ocean reanalysis temperature and salinity data (Balmaseda et al., 2013). The original Lombard et al. (2009, 2011)

5   equations are based upon a synthesis of culture studies, pooled together irrespective of experimental design or rationale, therefore they can be considered to conceptually represent the fundamental niche of a given foraminiferal species, *i.e.* the range in environment that the species can survive. Using the MARGO core top $\delta^{18}O_c$ database (MARGO Project Members*, 2009), Roche *et al.* (2018) computed the optimum depth habitat (the depth habitat that exhibits the strongest correlation when comparing FAME $\delta^{18}O_c$ and MARGO $\delta^{18}O_c$) for each species in the MARGO database (MARGO Project Members*,

10   2009). The MARGO database does not include *N. dutertrei,* meaning that we concentrate our efforts mainly on *G. ruber* and *G. sacculifer*. By identifying the optimum depth habitat, Roche *et al.* (2018) established the realised niche, *i.e.* the range in environment that the species can be found, for these species for the late Holocene. Unlike some foraminiferal models, FAME does not include limiting factors such as competition, respiration or predation variables as no reliable proxy exists for such parameterisation in the geological record, therefore aspects such as interspecific competition that may limit the niche width

15   of a species are not computed. Consequently, we allow all the species of foraminifera to grow down to ~ 400 m (depending if optimal temperature conditions are met) to capture the total theoretical niche width. As the optimised depths of Roche *et al.* (2018) are shallower, and upper ocean water is more prone to temperature variability, our approach likely dampens both the modelled $\delta^{18}O_c$ and T_c. Therefore, the sensitivity of the model was tested by applying the same procedure but with the limitation of the depth set to 60; 100 and 200 m.

20   **2. Methods**

2.1 Input variables (temperature; salinity and $\delta^{18}O_{sw}$)

The temperature and salinity of the ocean reanalysis data product (Universiteit Hamburg, DE) ORA S4 (Balmaseda et al., 2013) were extracted at one-degree resolution for the tropical Pacific (-20°S to 20°N and 120°E to -70°W), with each single grid cell comprised of data for 42 depth intervals (5 – 5300 m water depth) and 696 months (January 1957 – December

25   2015). A global 1-degree grid was generated, and each grid cell was classified as belonging to one of 27 distinct ocean regions, as defined by either societal and scientific agencies, for identifying regional $\delta^{18}O_{sw}$ – salinity relationships (LeGrande and Schmidt, 2006). Using the $\delta^{18}O_{sw}$ database of LeGrande and Schmidt (2006) a regional $\delta^{18}O_{sw}$ – salinity relationship was defined, of which the salinity is the salinity measured directly at the isotope sample collection point (included within the database). Two matrices were computed; one giving values of the slope (*m*) and the other of intercept

30   (*c*) of the resultant linear regression equations, these were used as look-up tables to define the monthly $\delta^{18}O_{sw}$ from the monthly salinity Ocean reanalysis product ORAS S4 (Balmaseda et al., 2013), which was used for the calculation of $\delta^{18}O_{eq,}$

i.e. the expected $\delta^{18}O$ for foraminiferal calcite formed at a certain temperature (Kim and O'Neil, 1997). The $\delta^{18}O_{eq}$ is calculated from a rearranged form of the following temperature equation:

$$T = T_0 - b \cdot (\delta^{18}O_c - \delta^{18}O_{sw}) + a \cdot (\delta^{18}O_c - \delta^{18}O_{sw})^2 \text{ , (1)}$$

Specifically, we used the quadratic approximation (Bemis et al., 1998) of Kim and O'Neil (1997), where T_0 = 16.1, a = 0.09,

5   b = -4.64 and converted from V-SMOW to V-PDB using a constant of -0.27 ‰ (Hut, 1987; Roche et al., 2017):

$$\Delta = b^2 - 4a \cdot (T_0 - T_{sw}) \text{ , (2)}$$

$$\delta^{18}O_{c,eq} = \frac{-b - \sqrt{\Delta}}{2a} + \delta^{18}O_{sw} - 0.27 \text{ , (3)}$$

2.2 Foraminifera as modelled entities (FAME)

For each latitude and longitude grid, a monthly growth rate was calculated using the ORA S4 temperature and a Michaelis-

10   Menton kinetics to predict growth calculated from culture experiments, described in Lombard et al. (2009). Growth rate was artificially constrained to arbitrary values of the upper 60; 100; 200 and 400 m for all species to reflect the symbiotic nature of various foraminiferal species. FAME is based upon FORAMCLIM which can compute eight foraminiferal species (Kageyama et al., 2013; Lombard et al., 2009, 2011; Roche et al., 2017), however comparison with a core top database has been limited to five foraminiferal species (Roche et al., 2017). Here the output of FAME is further restricted to three species

15   that have been the main focus of foraminifera-based studies that have been used to infer ENSO variability, namely the upper ocean dwelling *Globigerinoides sacculifer* and *Globigerinoides ruber*, as well as the thermocline dwelling *Neogloboquadrina dutertrei* (Ford et al., 2015; Koutavas et al., 2006; Koutavas and Joanides, 2012; Koutavas and Lynch-Stieglitz, 2003; Leduc et al., 2009; Sadekov et al., 2013).

2.3 Monthly growth rate (GR) weighted $\delta^{18}O$ and T_C

20   The FAME growth rate output was used to compute the monthly depth-weighted oxygen isotope distribution ($\sum_{z=0}^{zb(k)} \delta^{18}O_c$, where z is the depth) for each species, using the computed $\delta^{18}O_{eq}$ for a given latitudinal and longitudinal grid point, where $zb(k)$ is either 60; 100; 200 or 400 m. No correction for species specific disequilibria, such as vital effect, was applied to the data. At each grid point the total growth rate ($\sum_{t=1}^{nt} \sum_{z=0}^{zb(k)} GR$, where nt is the number of time steps) was calculated and each individual monthly growth rate ($\sum_{z=0}^{zb(k)} GR$) normalised to this value. A weighted histogram was constructed from the

25   corresponding oxygen isotope values (Figure S1), which will sum to 1 (or 100 %). The rationale for constructing a (flux/GR-)weighted histogram is related to the probability of an oxygen isotope value occurring, essentially for an unweighted distribution this is $p(\delta^{18}O_{v_i}) = \frac{c_i}{t}$, with each month contributing $\frac{1}{t}$ and therefore, having a maximum value for c_i of t (= 696). However, in reality the monthly contribution, if remineralisation of the settling flux and benthic seafloor processes (Lougheed et al., 2018) are for now largely ignored, is modulated by various hydrographic processes and related to the

30   temperature sensitivity (Jonkers and Kučera, 2017; Mix, 1987). Although other processes may also impact species such as

mixed layer depth and nutrients these for now can be ignored. Therefore, both the resultant $\delta^{18}O_c$ and flux are sufficiently perturbed/altered by T°C that for a weighted distribution each monthly contribution is $\frac{\sum_{z=0}^{zb(k)} GR}{\sum_{t=1}^{nt} \sum_{z=0}^{zb(k)} GR}$. The same procedure was executed for the T_c, where the computed $\delta^{18}O_{eq}$ is replaced with the ORA S4 temperature profile for a given latitudinal and longitudinal grid point.

2.4 Statistical analysis

The tropical Pacific Ocean is divided into four Niño regions based on historical ship tracks, from east to west: Niño 1 and 2 (0° to -10°S, 90°W to 80°W), Niño 3 (5°N to -5°S, 150°W to 90°W), Niño 3.4 (5°N to -5°S, 170°W to 120°W) and Niño 4 (5°N to -5°S, 160°E to 150°W). One index for ENSO, the Oceanic Niño Index (ONI), based upon the Niño 3.4 region (because of the region's importance for interactions between ocean and atmosphere) is a 3-month running mean of SST anomalies in ERSST.v5 (Huang et al., 2017). However, Pan-Pacific meteorological agencies differ in their definition (An and Bong, 2016, 2018) of an El Niño, with each country's definition reflecting socio-economic factors, therefore, for simplicity we utilise a threshold of $\chi \geq +0.5$°C as a proxy for El Niño, -0.5°C $\leq \chi \geq +0.5$°C for neutral climate conditions and -0.5°C $\leq \chi$ for a La Niña in the Oceanic Niño Index. Many meteorological agencies consider that five consecutive months of $\chi \geq +0.5$°C must occur for the classification of an El Niño event. However, here it is considered that any single month falling within our threshold values as representative of El Niño, neutral or La Niña conditions (grey bars in Figure 1). By using this threshold, three weighted histograms for each $\delta^{18}O_c$ and T_c and their resultant distributions (El Niño; Neutral; and La Niña) were computed for every month and for every latitude and longitude grid-point for the 1958-2015 period.

Monthly output representing different climate conditions were compared against each another for $\delta^{18}O_c$ and T_c separately. An Epanechnikov-kernel distribution was first fitted to the monthly output, after which any two desired distributions could be compared for similarity using an Anderson-Darling test. The areas where the two distributions are found to agree, at the 5% significance level, are shown as, e.g., the grey/white area in Figure's 3 to 6. Comparison, between the weighted $\left(p\left(\delta^{18}O_{v_i} \right) = \frac{\sum_{z=0}^{zb(k)} GR}{\sum_{t=1}^{nt} \sum_{z=0}^{zb(k)} GR} \right)$ and unweighted $\left(p\left(\delta^{18}O_{v_i} \right) = \frac{c_i}{t} \right)$ distributions were made for El Niño climate; combined Neutral and La Niña climates; only Neutral climate; and only La Niña climate.

As the weighted distributions are effectively probability distributions, in order to fit a distribution, we multiplied the bin counts by 1000, effectively converting probability into a hypothesised distribution. Using the repeat matrix function (MatLab function: *repmat*), a matrix of $\delta^{18}O_c$ was produced using each bin's mid-point ($\delta^{18}O_{mid-point}$) there is a threefold error combined with this methodology which may account for minor variation between discrete runs of the model: first the counts values were rounded to whole integers so an exact number of cells could be added to a matrix; secondly the $\delta^{18}O_{mid-point}$ was used which gives an error associated with the bin size (±0.05 ‰) that is symmetrical close to the distributions measures of central tendency but asymmetrical at the sides; and finally, the associated rounding error at the bin edges within a histogram (±0.005 ‰).

3.0 Results

3.1 FAME Output

Using a basin-wide statistical test, we examine whether the mean $\delta^{18}O_c$ values of a given El Niño foraminifera population (FP_{EN}) and a given non-El Niño ('Neutral conditions') foraminifera population (FP_{NEU}) can be expected to be significantly

5　different at any given specific location. Where FP_{EN} and FP_{NEU} exhibit significantly different mean $\delta^{18}O_c$ values, ENSO events can potentially be detected by paleoceanographers and unmixed using, for example, a simple mixing algorithm with individual foraminiferal analysis (Wit et al., 2013). In cases where FP_{EN} and FP_{NEU} do not exhibit significantly different means, then the chosen species and/or location represent a poor choice to study ENSO dynamics. We compute growth-weighted $\delta^{18}O_c$ (Figure 3 and 5) and temperature (Figure 6) distributions for each 1° by 1° grid cell in the fifty-eight year

10　simulation using FAME (Roche et al., 2018), constraining the calculation to the Tropical Pacific Ocean (between -20°S to 20°N and 120°E to -70°W).

Our model produces 696 individual monthly maps for all three species (Figure 2), a series of species-specific histograms for different climatic states for each grid-point (Figure S1) and their underlying cumulative distribution functions (Figure S2). While two of the three species (*G. ruber* and *G. sacculifer*) have similar ecologies, they show differences in their resultant

15　$\delta^{18}O_c$ for the same ocean conditions. These results can subsequently be compared to the recorded climate conditions associated with each grid cell and simulation time step: identification of timesteps that represent El Niño (EN), Neutral (NEU), and La Niña climate conditions was done using the Oceanic Nino Index (ONI) derivative (Huang et al., 2017) (Figure 1). Comparison, for each species, FAME's predicted growth-weighted $\delta^{18}O_c$ distributions associated with each climate event was done using an Anderson-Darling (AD) test. This statistical test can be used to determine whether or not

20　two distributions can be said to come from the same population. Our results show that much of the Pacific Ocean can be considered to have statistically different population between FP_{EN} and FP_{NEU}. We consider that the likely cause for such a remarkable result is due to FAME computing a weighted average and, therefore, the lack of a signal found exclusively within the regions demarked in Figure 1 as El Niño regions could represent how the temperature signal is integrated via an extension of the growth rate; growing season and depth habitat of distinct foraminiferal populations. To determine how

25　robust these results are we use the 1σ values of the observed (FAME) minus expected (MARGO), as computed by Roche et al. (2018) with the MARGO core top $\delta^{18}O_c$ database, as the potential error associated with the FAME model. We have computed regions in which the difference in oxygen isotopes between the two populations ($\Delta\delta^{18}O_c$) compared with the AD-test is smaller than the aforementioned error (Hatching in Figures 3 and 4), *i.e.* where the mean difference between FP_{EN} and FP_{NEU} is within the error. The hatched regions in Figure 3 considerably reduce the areal extent of significant difference

30　between FP_{EN} and FP_{NEU}, with the remaining regions aligning with the El Niño 3.4 region (Figure 1). No such test was performed on the *N. dutertrei* dataset, because of its absence from the MARGO dataset. However, *N. dutertrei* areas may be unsuitable for the extraction of a palaeoclimate signal for sedimentological reasons, as will be outlined later.

The model-driven results were assessed with the underlying observational dataset, to check if they consistent the input data (temperature and $\delta^{18}O_{eq}$) underwent the same statistical test (Figure 4 and Figure S3). Instead of a variable depth, we opted for fixed depths at 5, 149 and 235 m, giving a Eulerian view (Zhu et al., 2017a) in which to observe the implications of a dynamic depth habitat. By using a fixed depth, these results show that the shallowest depths produce populations that are

5 significantly different both in terms of their mean values and their distributions. In the upper panel of Figure 4, the canonical El Niño 3.4 region is clearly visible at 5 m depth. Whilst differences exist between the temperature (Figure 4) and the FAME AD results (Figure 3), for instance close to the Panama isthmus, there are significant similarities between the plots. These plots also show that our FAME data (Figure 3), in which we allow foraminiferal growth down deeper than the depths in Roche et al. (2018), are a conservative estimate and thus are on the low-end (Figure 4), to account for potential discrepancies

10 with depth habitats. In the original paper on depth habitats based upon temperatures derived from $\delta^{18}O_c$, Emiliani (1954) cautioned that the depth habitats obtained would represent a weighted average of the total population, and while foraminiferal depth habitats are likely to vary spatiotemporally, the average depth habitat is skewed toward the dominant signal (Mix, 1987).

To further test the model-driven results and to assess if they are still consistent when the depth limitation (400 m) is shoaled

15 (to 60, 100, 200 m), the analysis was rerun with the aforementioned range of depths (Figure 5 and 6). Whilst it is possible to discern differences between the depths, it is important to note that a large percentage of the tropical Pacific remains accessible to palaeoclimate studies. A shallower depth limitation in the model increases the area for the 'warm' species, suggesting that the influence of a reduced variability in temperature or $\delta^{18}O_{eq}$ with a deeper depth limit causes the differences between FP_{EN} and FP_{NEU} to be reduced.

20 ## 3.2 Water depth and SAR

The resolution of the ocean reanalysis data for the time period 1958-2015 would essentially be analogous with a sediment core representing 50 yr^{-1} cm^{-1} (or 20 cm^{-1} kyr^{-1}). Based on our analysis, such a hypothetical core with a rapid sediment accumulation rate (SAR) could allow for the possible disentanglement of El Niño related signals from the climatic signal using IFA, but only in a best-case scenario involving minimal bioturbation, which is unlikely in the case of oxygenated

25 waters. Indeed, one should view discrete sediment intervals, and the foraminifera contained within them, as representative of an integrated multi-decadal or even multi-centennial signal (Lougheed et al., 2018; Peng et al., 1979), as opposed to other proxies such as corals (Cole and Tudhope, 2017), speleothems (Chen et al., 2016), or varves in which distinct layers correspond to discrete time intervals (true 'time-series' proxies). Therefore, in order to reliably extract short-term environmental information from foraminiferal-based proxies, the signal that one is testing or aiming to recover must exhibit

30 a large enough amplitude in order to perturb the population by a significant degree from the background signal, otherwise it will be lost due to the smoothing effect of bioturbation (Hutson, 1980a; Löwemark, 2007; Löwemark et al., 2005, 2008; Löwemark and Grootes, 2004) upon the downcore, discrete-depth signal (Cole and Tudhope, 2017; Mix, 1987). Similarly, the individual characters of El Niño events, which are very short in duration, become lost in the bioturbated sediment record.

New geochronological tools, such as dual ^{14}C-δ^{18}O measurements on single foraminifera (Lougheed et al., 2018), show that low sedimentation rate cores can have large variances in age between individual foraminifera present within a discrete 1 cm depth interval (Berger and Heath, 1968; Lougheed et al., 2018). In the case of a high SAR core (20 cm^{-1} kyr^{-1}), assuming a sediment mixing layer of 10 cm, benthic seafloor processes would result in a minimum 700-year 1σ confidence interval for a

5   1 cm discrete depth age (Lougheed et al., 2018). A consequence of bioturbation in sediment cores is that a series of high magnitude, but low frequency El Niño events could be smoothed out of the downcore, discrete-depth record. To investigate which areas of the sea floor can potentially preserve a foraminiferal downcore signal, we overlay our results with a map of time-averaged deep-sea SAR (Olson et al., 2016), adapted by Lougheed *et al.* (2018) to also show seafloor areas under the CCD depth, where carbonate material is not preserved(Berger, 1967, 1970b). Of the total area where FP_{EN} is significantly

10 different from FP_{NEU} (*i.e.* those areas where planktonic foraminiferal flux is suitable for reconstructing past ENSO dynamics), only a small proportion corresponds to areas where the sea floor is both above the CCD (< 3500 mbsl) and SAR is at least 5 cm/ka (Figure 3D). Also of note is that fact that much of the canonical El Niño 3.4 region (Wang et al., 2017) used in oceanography (Figure 1) is also excluded from these suitable areas in Figure 3D.

4.0 Discussion

15 ### 4.1 Palaeoceanographic Implications

Palaeoceanographic (Ford et al., 2015; Garidel-Thoron et al., 2007; Koutavas et al., 2006; Koutavas and Joanides, 2012; Koutavas and Lynch-Stieglitz, 2003; Leduc et al., 2009; Sadekov et al., 2013; White et al., 2018) and palaeoclimatological archives (Moy et al., 2002) have been used to indirectly and directly study past ENSO. Several authors have focussed on individual foraminifera analysis (IFA) or pooled foraminiferal analysis in the Pacific region, either for trace metal or stable

20 isotope geochemistry. Given the complexity in reconstructions of trace metal geochemistry (Elderfield and Ganssen, 2000; Nürnberg et al., 1996), and the potential error associated with determining which carbonate phase is first used when foraminifera biomineralise (Jacob et al., 2017), the focus here has been on the δ^{18}O$_c$. The resultant data of such studies have been used to infer a relatively weaker Walker circulation, a displaced ITCZ and equatorial cooling (Koutavas and Lynch-Stieglitz, 2003); both a reduction (Koutavas and Lynch-Stieglitz, 2003) and intensification (Dubois et al., 2009) in eastern

25 equatorial Pacific upwelling; and both weakened (Leduc et al., 2009) and strengthened ENSO variability (Koutavas and Joanides, 2012; Sadekov et al., 2013) during the LGM. A number of these results are contentious, for instance the reduction in upwelling in this region (Koutavas and Lynch-Stieglitz, 2003) is contradicted by Dubois et al. (2009), who used alkenones (i.e., $U_{37}^{K'}$ ratios) to suggest an upwelling intensification. Whilst the $U_{37}^{K'}$ proxy has problems within coastal upwelling sites (Kienast et al., 2012) it does not discount their claim, especially considering that δ^{18}O records can themselves be influenced

30 by salinity upon the δ^{18}O$_{sw}$ component (Rincón-Martínez et al., 2011) and the potential influence of [CO$_3$$^{2-}$] upon foraminiferal δ^{18}O$_c$ (de Nooijer et al., 2009; Spero et al., 1997; Spero and Lea, 1996). Furthermore, the discrepancies between marine cores' is worth noting, especially considering that terrestrial records suggest the number of El Niño events

per century in the early Holocene (8-6 ka BP) was minimal (Moy et al., 2002), with between 0 and 10 events occurring per century. This dampened ENSO is observed within lake core colour intensity and records driven primarily by precipitation (Cole and Tudhope, 2017; White et al., 2018). If the number and magnitude of ENSO events were reduced, the relatively low downcore resolution of marine records may not accurately capture the dynamics of such lower amplitude ENSO events

5 using existing methods. The possibility of a marine sediment archive being able to reconstruct ENSO dynamics comes down to several fundamentals: the time-period captured by the sediment intervals (a combination of SAR and bioturbation), the frequency and intensity of ENSO events, as well as the foraminiferal abundance during ENSO and non-ENSO conditions.

The results presented here imply that much of the Pacific Ocean is not suitable for reconstructing ENSO studies using
10 palaeoceanography, yet several studies have exposed shifts within $\sigma(\delta^{18}O_c)$ of surface and thermocline dwelling foraminifera. One can, therefore, question what is being reconstructed in such studies. One artefact of sampling is the potential occurrence of aliasing (Pisias and Mix, 1988; Wunsch, 2000; Wunsch and Gunn, 2003): a fundamental problem with proxy records is that they can be confounded by local regional climate, and/or ENSO's teleconnections, that mimic ENSO changes albeit at a different temporal frequency (Dolman and Laepple, 2018). Our own analysis using our FAME
15 $\delta^{18}O_c$ and T_c output mimics foraminiferal sedimentary archives, pooling several decades worth of data in which the resolution is coarse enough to obscure and prevent individual El Niño events being visible but allowing for some kind of long-term mean state of ENSO activity to be reconstructed (Cole and Tudhope, 2017). The results of our Anderson-Darling test may be unduly influenced by the Pacific decadal variability (PDV), also referred to as the Pacific Decadal Oscillation (PDO) (Pena et al., 2008). In much of the tropical Pacific the ratio of decadal to interannual σSST suggests that they are
20 comparable in magnitude, therefore fluctuations in SST are more obviously apparent outside of the purely canonical regions of ENSO (Wang et al., 2017). It could be that the areas outside of these canonical ENSO regions (Figure 1) reflect the PDO (Pena et al., 2008; Wang et al., 2017). The use of $\sigma(\delta^{18}O_c)$ as an indicator of ENSO is dependent on whether the variance is dominated by interannual variance (Ford et al., 2015; Thirumalai et al., 2013; Zhu et al., 2017a). Zhu *et al.* (2017) computed the total variance change with and without the annual cycle suggesting that, for some cores the increased assumed ENSO
25 variability at the LGM as deduced by proxy records (Koutavas et al., 2006; Koutavas and Joanides, 2012; Koutavas and Lynch-Stieglitz, 2003) may be purely a by-product of the annual cycle.

4.2 Limitations of the methods applied and assessment of model uncertainties

For simplicity we have assumed that our model is 'perfect', of course that is inaccurate, there are four potential sources of error: the input variables (temperature, salinity and their conversion into $\delta^{18}O_{sw}$ and $\delta^{18}O_{eq}$); the model's error with respect to
30 real world values (Roche et al., 2018); the statistical test's errors (associated Type I – in which attribution of significance is given to an insignificant random event, a false 'positive' – and Type II – in which a significant event is attributed to be insignificant, a false 'negative' - errors); and reducing the complexities of foraminiferal biology via parameterization. The input variables can have errors associated with both the absolute values of temperature and salinity used here; and the

limitation of input values to a single value per month. Whilst it is possible to interpolate to a daily resolution, this is problematic for two reasons: (1) daily temperature records have much more high frequency oscillations than the data here and (2) the lifecycle of a single foraminifera is approximately monthly, therefore by using monthly data it provides an estimate of the average population signal. Conversion of salinity and temperature into $\delta^{18}O_{sw}$ and $\delta^{18}O_{eq}$ uses a quadratic

5 approximation, one source of error is the unknown influence of carbonate ion concentration on both the Kim and O'Neil (1997) equation and the foraminiferal microenvironment (de Nooijer et al., 2008, 2009; Spero et al., 1997; Spero and DeNiro, 1987; Spero and Lea, 1996) which has further implications due to the upwelling of cool, low pH, waters in the eastern Tropical Pacific (Cole and Tudhope, 2017; Raven et al., 2005). The spatial variability in salinity, particularly within regions underlying the intertropical convergence zone (ITCZ) and the moisture transport from the Caribbean into the eastern

10 Pacific along the topographic low that represents Panama Isthmus, the resultant conversion of salinity to $\delta^{18}O_{sw}$ and then $\delta^{18}O_{eq}$ may contain further error. If such errors are independent of the absolute value of the variable, *i.e.* the error on cold temperature is the same and not larger than warm temperatures, then the error terms effectively cancel one another out. A point of note, is that the $\delta^{18}O$ to °C conversion of Kim and O'Neil (1997) is considered to be marginally larger at the cold end then at the warm end (0.2 ‰ per 1°C to 0.22 ‰ per 1°C) than that originally discerned (O'Neil et al., 1969). The

15 comparison of the temperature signal produced here (T_c) to a value corresponding to that reconstructed from measurements of Mg/Ca should be done with caution. As stated previously, several other parameters can alter this technique, this includes abiotic effects such as salinity (Allen et al., 2016; Gray et al., 2018; Groeneveld et al., 2008; Kısakürek et al., 2008) or carbonate ion concentration (Allen et al., 2016; Evans et al., 2018; Zeebe and Sanyal, 2002); biotic effects such as diurnal calcification (Eggins et al., 2003; Hori et al., 2018; Sadekov et al., 2008, 2009; Vetter et al., 2013); or additional factors such

20 as sediment (Fallet et al., 2009; Feldmeijer et al., 2013) or specimen (Barker et al., 2003; Greaves et al., 2005) 'cleaning' techniques. Given the role of Mg in inhibiting calcium carbonate formation, the manipulation of seawater similar to the modification of the cell's pH (de Nooijer et al., 2008, 2009) may aid calcification and explain the formation of low-Mg by certain foraminifera (Zeebe and Sanyal, 2002), however scaling these processes up to a basin-wide model is beyond the remit of this current paper.

25 Our modelling results also depend upon the species symbiotic nature and potential genotypes. For instance, mixotrophs, those organisms that utilise a mixture of sources for energy and carbon (planktonic foraminifera such as *G. ruber*; and/or *G. sacculifer*) can outcompete heterotrophic (or photoheterotrophic) organisms (planktonic foraminifera such as *N. pachyderma*; *N. incompta*) especially in stratified-oligotrophic waters. FORAMCLIM has placed both *G. bulloides* and *N. dutertrei* as symbiont barren for the purposes of ecophysiological parameters used for computing expected potential habitats for both

30 future and past scenarios. However, recent culture studies have shown that *G. bulloides* Type IId instead of being symbiont barren actually plays host to endobiotic cyanobacteria (Bird et al., 2017), whilst *N. dutertrei* Type Ic contains what are reputed to be algal symbionts (Bird et al., 2018). They do however, confirm that *N. incompta* is symbiont barren (Bird et al., 2018). The authors have suggested that ecophysiological models, such as FORAMCLIM, should be updated to include both the photosynthetic changes and resultant respiration parameters (Bird et al., 2018). Whilst FAME uses only the temperature

component of FORAMCLIM (Roche et al., 2018) and we have only modelled *N. dutertrei*, it is important to note that there are distinctions between the fundamental niche that FAME computes, *i.e.* the conditions that an organism can survive, and the realised niche, *i.e.* what an organism actually occupies given limiting factors within the environment. Likewise, FAME and FORAMCLIM are based upon the original culture experiments that assumed that both species (*G. bulloides* and *N.*
5   *dutertrei*) are non-symbiotic. A species that hosts symbionts will likely have a restricted temperature that is associated with the temperature tolerance of their symbionts, given that the next geneartion of a species of planktonic foraminifera must be re-infected with their symbionts. Variation in cryptic species of *G. bulloides* do exist, given that genotypes of morphotypes exhibit distinct environmental preferences (Darling et al., 2000, 1999; Huber et al., 1997; Morard et al., 2013; de Vargas et al., 1999, 2002), especially between genotypes Type Ia, Ib, IIa, IIb, and IIc and the genotype Type IId that has a restricted
10 geographic distribution (Darling et al., 2004). Morard *et al.* (2013) simulated the impact of genotypes upon palaeoceanographic reconstructions (in particular transfer functions) using a theoretical abundance, calculated with a best-fit gaussian response model, depending upon SST later using a similar approach (Morard et al., 2016) to deduce the impact upon $\delta^{18}O$. Incorporation of both a theoretical genotype abundance (Morard et al., 2013) and ecophysiological tolerances of different genotypes (Bird et al., 2018) within an ecophysiological model could further reduce error within modelling of
15 planktonic foraminiferal habitats, and thus reduce data-model comparison error.

Conclusion

Previous work has focussed on comparing either the difference between time slices or between downcore and modern IFA variance, using a reduction in $\sigma(\delta^{18}O_c)$ as an indicator of reduced ENSO (Zhu et al., 2017a). Concentrating on the period spanning the instrumental record by using the FAME module, we present a species-specific $\delta^{18}O$ and Temperature output
20 (T_c) for ocean reanalysis data to validate the use of foraminiferal proxies in reconstructing ENSO dynamics in the Pacific Ocean. Overall, our results suggest that foraminiferal $\delta^{18}O$ for a large part of the Pacific Ocean can be used to reconstruct ENSO, especially if an individual foraminiferal analysis (Lougheed et al., 2018; Wit et al., 2013) approach is used (Ford et al., 2015; Koutavas et al., 2006; Koutavas and Joanides, 2012; Koutavas and Lynch-Stieglitz, 2003; Sadekov et al., 2013; White et al., 2018), contrary to previous analysis (Thirumalai et al., 2013). However, the sedimentation rate of ocean
25 sediments in the region is notoriously slow (Olson et al., 2016) and much of the ocean floor is under the CCD. These factors reduce the size of the area available for reconstructions considerably (Lougheed et al., 2018), thus precluding the extraction of a temporally valid palaeoclimate signal using long-standing methods. We further highlight that the conclusions drawn from foraminiferal reconstructions should consider both the frequency and magnitude of El Niño events during the corresponding sediment time interval (with full error) to fully understand whether or not a strengthening or dampening
30 occurred. The use of ecophysiological models (Kageyama et al., 2013; Lombard et al., 2009, 2011) are not limited to foraminifera and provide an important way to test whether proxies used for palaeoclimate reconstructions are suitable for the given research question.

Code and data availability

The ocean reanalysis data used in this paper are available from the Universiteit Hamburg, an open source version of FAME code is available from Roche et al. (2018), and the statistical routines are available as part of the Statistical package of MATLAB R2018a. A video of the $\delta^{18}O_{shell}$ output has been archived online (https://doi.org/10.5281/zenodo.2554843,

5   Metcalfe et al., 2019).

Author Contributions

B.M. and D.M.R. designed the study. B.M. analysed the data. B.C.L. processed ocean SAR and depth data. B.M. drafted the manuscript with contributions from all authors.

Competing Interests

10   The authors declare no competing interests.

Acknowledgements
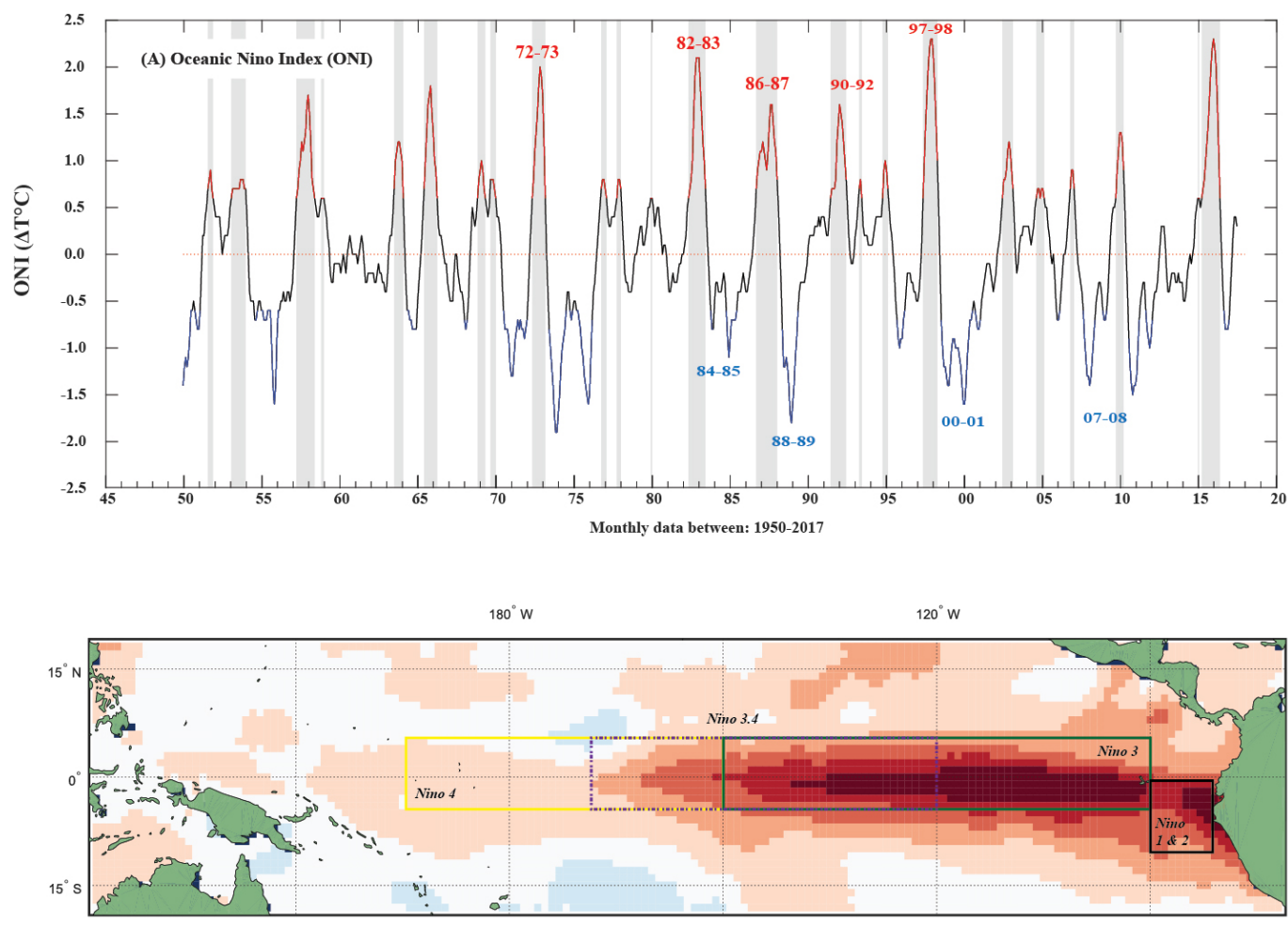
Figure 1. Oceanic Niño Index and the temperature anomaly for a single El Niño event. (Top) Oceanic Niño Index (ONI), sourced from a 3-month running mean of SST anomalies in ERSST.v5 of the Niño 3.4 region (Huang et al., 2017). Grey vertical bars represent the periods in which El Niño-like conditions exist using a simple one-month threshold. (Bottom) The sea surface temperature difference between week beginning 1st December 1997 minus the long-term climatic mean (1971 – 2000) for December. The 1997 – 1998 El Niño represents an EP-ENSO. The long term monthly climatology, the NOAA optimum interpolation (OI) SST V2, based upon the methodology of Reynolds and Smith (Reynolds and Smith, 1995) using two distinct climatologies for 1971 - 2000 and 1982 – 2000 (Reynolds et al., 2002). Boxes represent the Nino region: Niño 1 and 2 (0° - -10°S, 90°W - 80°W), Niño 3 (5°N - -5°S, 150°W - 90°W), Niño 3.4 (5°N - -5°S, 170°W - 120°W) and Niño 4 (5°N - -5°S, 160°E - 150°W).
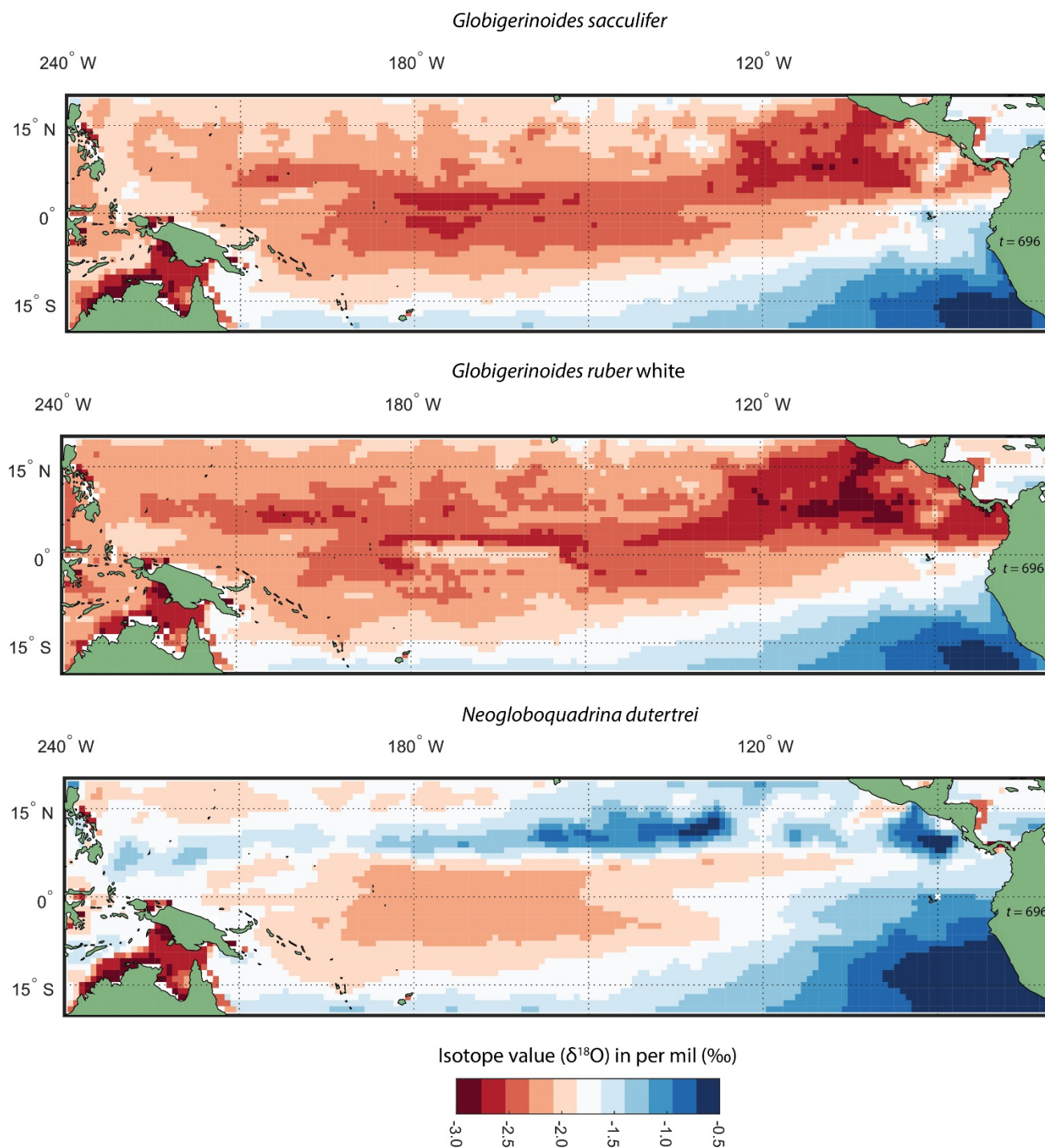
Figure 2. A snapshot of the output of FAME. Each panel represents an individual species (Top Panel *G. sacculifer*; Middle Panel *G. ruber* and Bottom Panel *N. dutertrei*) $\delta^{18}O$ for a single time step (t = 696). The $\delta^{18}O$ for each grid-point is based upon FAME, a computed integrated signal based upon the growth rate and the $\delta^{18}O_{eq}$ values. Values in per mil (‰ V-PDB).
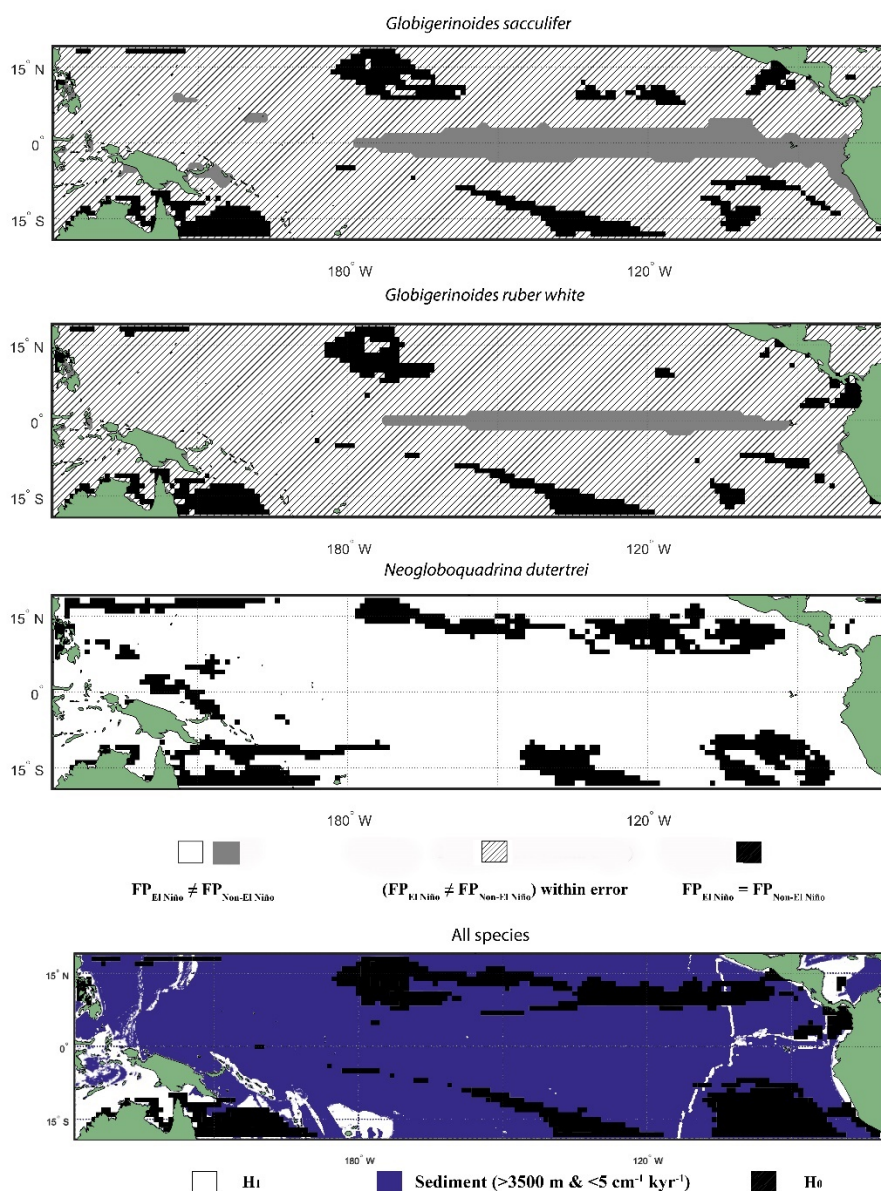
Figure 3. Maps of those locations that can reconstruct El Niño events for *G. ruber*; *G. sacculifer*; *N. dutertrei* and all species. Upper (three) panels represent the Anderson-Darling test results for the species *G. ruber*; *G. sacculifer*; and *N. dutertrei* where the black areas reflect latitudinal and longitudinal grid points that failed to reject the null hypothesis (H_0) and therefore the foraminiferal population (FP) of the El Niño is similar to the Non-El Niño, and therefore the distribution between the neutral climate and El Nino cannot be said to be different ($FP_{El\ Niño} = FP_{Non-El\ Niño}$). White/grey areas reflect regions in which the H_1 hypothesis is accepted, therefore the distributions can be said to be unique ($FP_{El\ Niño} \neq FP_{Non-El\ Niño}$). Hatching represents the FAME species specific values of 0.32 ‰ and 0.20 ‰. The final, bottom, panel represents a synthesis of the upper panels areas in which reconstructions are possible, represented by both the blue and white area. The black area represents those areas where the null hypothesis for all three species cannot be rejected. Blue represents sedimentological limitations that preclude the extraction of a foraminiferal signal from the sediment: deeper than 3500 mbsl (below CCD) and time averaged sediment accumulation rate (SAR) of less than <5 cm/ka (Lougheed et al., 2018; Olson et al., 2016) (see Figure S7 for the different sedimentological components).
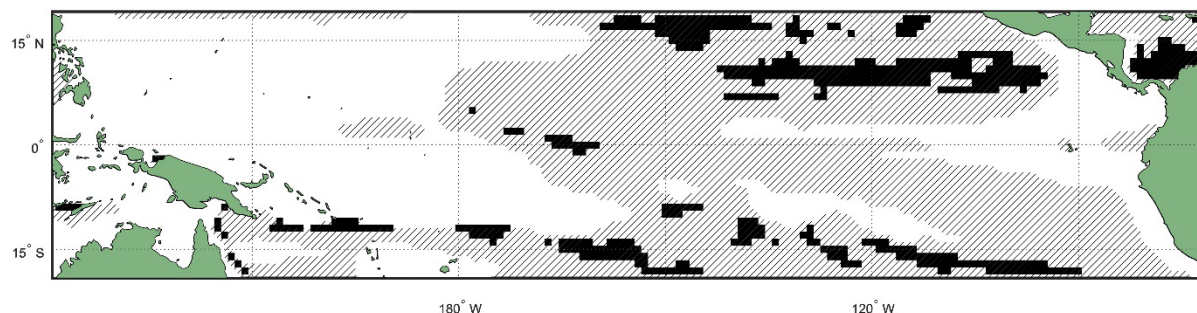
16
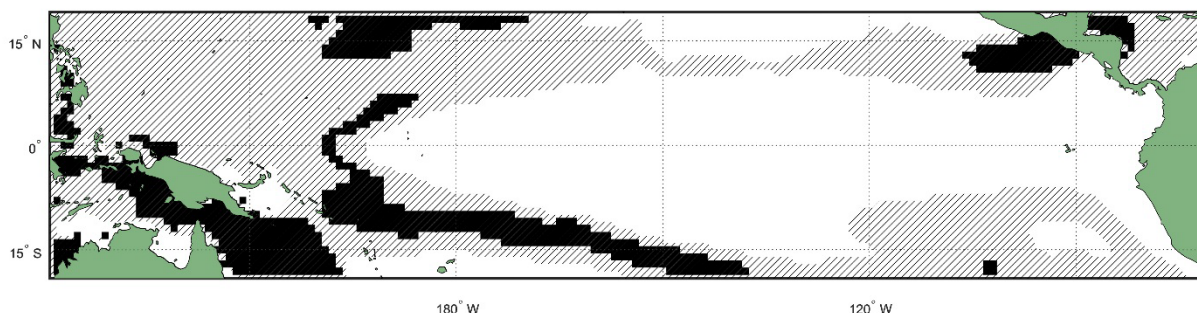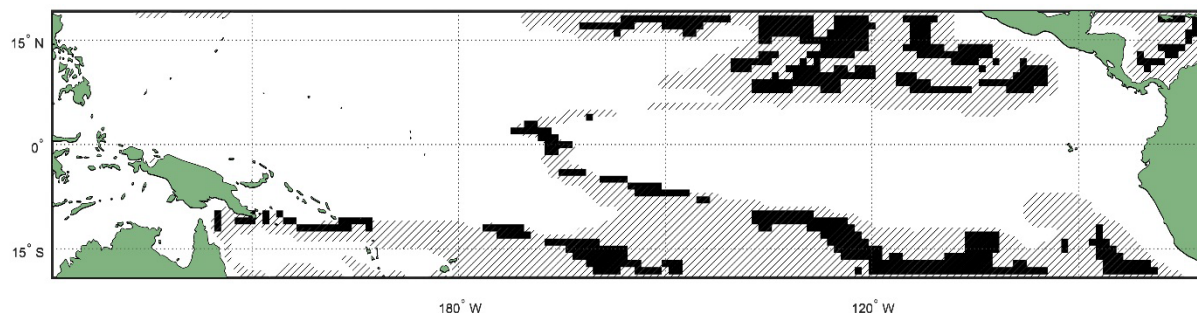
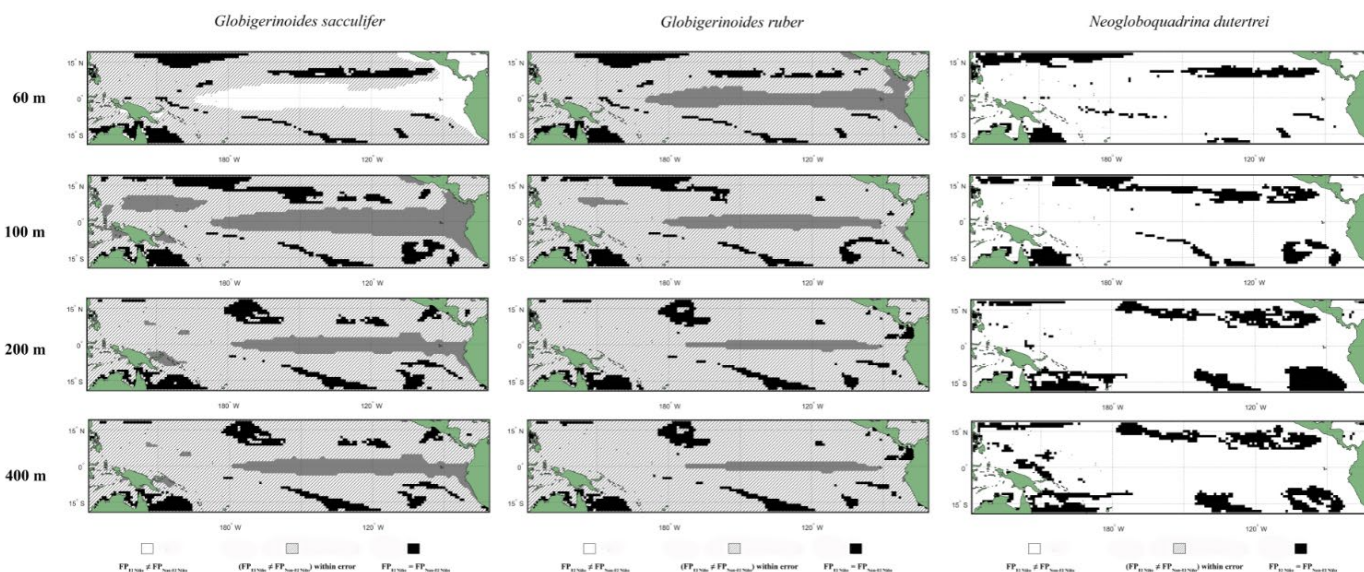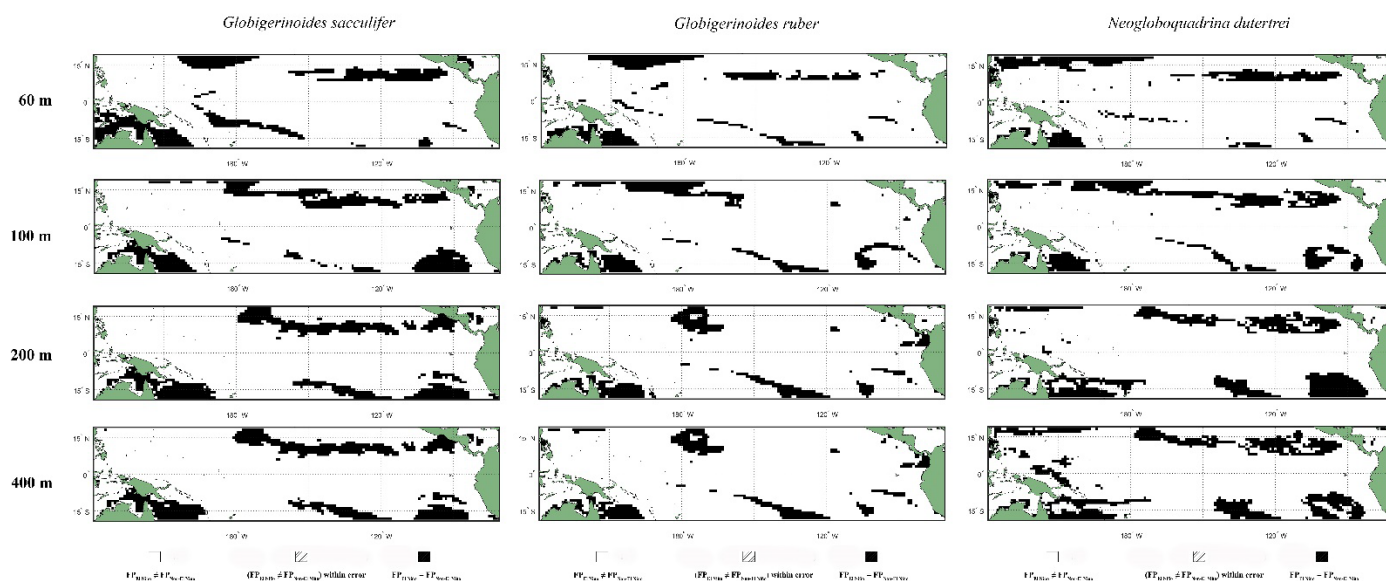**Figure 4. Results of an Anderson-Darling test between El Nino and Neutral climate conditions based upon the Temperature input data: Fixed depth. White represents where the H_1 hypothesis is accepted, therefore the distributions of the foraminiferal population (FP) for El Niño and Non- El Niño can be said to be unique ($FP_{El Niño} \neq FP_{Non-El Niño}$). Black that the null hypothesis (H_0), that the El Niño and Non- El Niño populations are not statistically different ($FP_{El Niño} = FP_{Non-El Niño}$), cannot be rejected. The hatching represents those locations where the difference between the means of both populations is less than 0.5°C. Each panel represents a single depth (5, 150 and 250 m) sampled equally through time.**

Figure 5. Oxygen isotope (δ¹⁸O_c): Maps of those locations that can reconstruct El Niño events for (Left Panel) *G. ruber*; (Middle panel) *G. sacculifer*; and (Right panel) *N. dutertrei*. Panels represent the Anderson-Darling test results for the species *G. ruber*; *G. sacculifer*; and *N. dutertrei* where the black areas reflect latitudinal and longitudinal grid points that failed to reject the null hypothesis (H₀) and therefore the foraminiferal population (FP) of the El Niño is similar to the Non-El Niño, and therefore the distribution between the neutral climate and El Nino cannot be said to be different (FP_El Niño = FP_Non-El Niño). White/grey areas reflect regions in which the H₁ hypothesis is accepted, therefore the distributions can be said to be unique (FP_El Niño ≠ FP_Non-El Niño). Hatching represents the FAME species specific values of 0.32 ‰ and 0.20 ‰. Each row represents a particular depth limit for the model, from top to bottom: 60 m; 100 m; 200 m and 400 m.

Figure 6. Temperature signal (T$_C$): Maps of those locations that can reconstruct El Niño events for (Left Panel) *G. ruber*; (Middle panel) *G. sacculifer*; and (Right panel) *N. dutertrei*. Panels represent the Anderson-Darling test results for the species *G. ruber*; *G. sacculifer*; and *N. dutertrei* where the black areas reflect latitudinal and longitudinal grid points that failed to reject the null hypothesis (H$_0$) and therefore the foraminiferal population (FP) of the El Niño is similar to the Non-El Niño, and therefore the distribution between the neutral climate and El Nino cannot be said to be different (FP$_{El Niño}$ = FP$_{Non-El Niño}$). White/grey areas reflect regions in which the H$_1$ hypothesis is accepted, therefore the distributions can be said to be unique (FP$_{El Niño}$ ≠ FP$_{Non-El Niño}$) Each row represents a particular depth limit for the model, from top to bottom: 60 m; 100 m; 200 m and 400 m.

References

Allen, K. A., Hönisch, B., Eggins, S. M., Haynes, L. L., Rosenthal, Y. and Yu, J.: Trace element proxies for surface ocean conditions: A synthesis of culture calibrations with planktic foraminifera, Geochimica et Cosmochimica Acta, 193, 197–221, doi:10.1016/j.gca.2016.08.015, 2016.

An, S.-I. and Bong, H.: Inter-decadal change in El Niño-Southern Oscillation examined with Bjerknes stability index analysis, Climate Dynamics, 47(3–4), 967–979, doi:10.1007/s00382-015-2883-8, 2016.

An, S.-I. and Bong, H.: Feedback process responsible for the suppression of ENSO activity during the mid-Holocene, Theoretical and Applied Climatology, 132(3–4), 779–790, doi:10.1007/s00704-017-2117-6, 2018.

Anderson, L., Abbott, M. B., Finney, B. P. and Edwards, M. E.: Palaeohydrology of the Southwest Yukon Territory, Canada, based on multiproxy   analyses of lake sediment cores from a depth transect, The Holocene, 15(8), 1172–1183, doi:10.1191/0959683605hl889rp, 2005.

Asmerom, Y., Polyak, V., Burns, S. and Rassmussen, J.: Solar forcing of Holocene climate: New insights from a speleothem record, southwestern United States, Geology, 35(1), 1–4, doi:10.1130/G22865A.1, 2007.

Balmaseda, M. A., Mogensen, K. and Weaver, A. T.: Evaluation of the ECMWF ocean reanalysis system ORAS4, Quarterly Journal of the Royal Meteorological Society, 139(674), 1132–1161, 2013.

Barker, S., Greaves, M. and Elderfield, H.: A study of cleaning procedures used for foraminiferal Mg/Ca paleothermometry, Geochem. Geophys. Geosyst., 4(9), 8407, 2003.

Barron, J. A. and Anderson, L.: Enhanced Late Holocene ENSO/PDO expression along the margins of the eastern North Pacific, Quaternary International, 235(1), 3–12, doi:https://doi.org/10.1016/j.quaint.2010.02.026, 2011.

Barron, J. A., Heusser, L., Herbert, T. and Lyle, M.: High-resolution climatic evolution of coastal northern California during the past 16,000 years, Paleoceanography, 18(1), doi:10.1029/2002PA000768, 2003.

Bé, A. W. H. and Spero, H. J.: Shell regeneration and biological recovery of planktonic foraminfera after physical injury induced in laboratory culture, Micropaleontology, 27(3), 305–316, 1981.

Bé, A. W. H., Spero, H. J. and Anderson, O. R.: Effects of symbiont elimination and reinfection on the life processes of the planktonic foraminifer Globigerinodies sacculifer, Marine Biology, 70, 73–86, 1982.

Bemis, B. E., Spero, H. J., Bijma, J. and Lea, D. W.: Reevaluation of the oxygen isotopic composition of planktonic foraminifera: Experimental results and revised paleotemperature equations, Paleoceanography, 13(2), 150–160, doi:10.1029/98PA00070, 1998.

Bennett, J. R., Cumming, B. F., Leavitt, P. R., Chiu, M., Smol, J. P. and Szeicz, J.: Diatom, Pollen, and Chemical Evidence of Postglacial Climatic Change at Big Lake, South-Central British Columbia, Canada, Quaternary Research, 55(3), 332–343, doi:10.1006/qres.2001.2227, 2001.

Benson, L., Kashgarian, M., Rye, R., Lund, S., Paillet, F., Smoot, J., Kester, C., Mensing, S., Meko, D. and Lindström, S.: Holocene multidecadal and multicentennial droughts affecting Northern California and Nevada, Quaternary Science Reviews, 21(4), 659–682, doi:https://doi.org/10.1016/S0277-3791(01)00048-8, 2002.

Berger, W. H.: Foraminiferal Ooze: Solution at Depths, Science, New Series, 156(3773), 383–385, 1967.

Berger, W. H.: Planktonic Foraminifera: Differential Production and Expatriation Off Baja California, Limnology and Oceanography, 15(2), 183–204, 1970a.

Berger, W. H.: Planktonic Foraminifera: Selective solution and the lysocline, Marine Geology, 8(2), 111–138, doi:10.1016/0025-3227(70)90001-0, 1970b.

Berger, W. H.: Sedimentation of planktonic foraminifera, Marine Geology, 11(5), 325–358, doi:10.1016/0025-3227(71)90035-1, 1971.

Berger, W. H. and Gardner, J. V.: On the determination of Pleistocene temperatures, Journal of Foraminiferal Research, 5(2), 102–113, 1975.

Berger, W. H. and Heath, G. R.: Vertical mixing in pelagic sediments, Journal of Marine Research, 26(2), 134–143, 1968.

Bijma, J., Hönisch, B. and Zeebe, R. E.: Impact of the ocean carbonate chemistry on living foraminiferal shell weight: Comment on "Carbonate ion concentration in glacial-age deep waters of the Caribbean Sea" by W. S. Broecker and E. Clark: COMMENT, Geochemistry, Geophysics, Geosystems, 3(11), 1–7, doi:10.1029/2002GC000388, 2002.

Bird, C., Darling, K. F., Russell, A. D., Davis, C. V., Fehrenbacher, J., Free, A., Wyman, M. and Ngwenya, B. T.: Cyanobacterial endobionts within a major marine planktonic calcifier (Globigerina bulloides, Foraminifera) revealed by 16S rRNA metabarcoding, Biogeosciences, 14(4), 901–920, doi:10.5194/bg-14-901-2017, 2017.

Bird, C., Darling, K. F., Russell, A. D., Fehrenbacher, J. S., Davis, C. V., Free, A. and Ngwenya, B. T.: 16S rRNA gene metabarcoding and TEM reveals different ecological strategies within the genus Neogloboquadrina (planktonic foraminifer), edited by F. Frontalini, PLOS ONE, 13(1), e0191653, doi:10.1371/journal.pone.0191653, 2018.

Boltovskoy, D.: The Sedimentary record of Pelagic Biogeography, Progress in Oceanography, 34(2–3), 135–160, 1994.

Boltovskoy, E.: 314. Depth at which foraminifera can survive in sediments, Contributions from the Cushman Foundation for Foraminiferal Research, XVII(2), 43–45, 1966.

Branson, O., Redfern, S. A. T., Tyliszczak, T., Sadekov, A., Langer, G., Kimoto, K. and Elderfield, H.: The coordination of Mg in foraminiferal calcite, Earth and Planetary Science Letters, 383, 134–141, doi:10.1016/j.epsl.2013.09.037, 2013.

Branson, O., Bonnin, E. A., Perea, D. E., Spero, H. J., Zhu, Z., Winters, M., Hönisch, B., Russell, A. D., Fehrenbacher, J. S. and Gagnon, A. C.: Nanometer-Scale Chemistry of a Calcite Biomineralization Template: Implications for Skeletal Composition and Nucleation, Proceedings of the National Academy of Sciences, 113(46), 12934–12939, doi:10.1073/pnas.1522864113, 2016.

Caley, T., Roche, D. M., Waelbroeck, C. and Michel, E.: Oxygen stable isotopes during the Last Glacial Maximum climate: perspectives from data–model (iLOVECLIM) comparison, Climate of the Past, 10(6), 1939–1955, doi:10.5194/cp-10-1939-2014, 2014.

Caramanica, A., Quilter, J., Huaman, L., Villanueva, F. and Morales, C. R.: Micro-remains, ENSO, and environmental reconstruction of El Paraíso, Peru, a late preceramic site, Journal of Archaeological Science: Reports, 17, 667–677, doi:https://doi.org/10.1016/j.jasrep.2017.11.026, 2018.

Chen, S., Hoffmann, S. S., Lund, D. C., Cobb, K. M., Emile-Geay, J. and Adkins, J. F.: A high-resolution speleothem record of western equatorial Pacific rainfall: Implications for Holocene ENSO evolution, Earth and Planetary Science Letters, 442, 61–71, doi:https://doi.org/10.1016/j.epsl.2016.02.050, 2016.

CLIMAP Project Members: The Surface of the Ice-Age Earth, Science, 191(4232), 1131–1137, 1976.

5 Cole, J. and Tudhope, A. W.: Reef-Based Reconstructions of Eastern Pacific Climate Variability, in Coral Reefs of the Eastern Tropical Pacific: Persistence and Loss in a Dynamic Environment, edited by P. W. Glynn, D. P. Manzello, and I. C. Enochs, pp. 535–548, Springer Netherlands, Dordrecht., 2017.

Conroy, J. L., Overpeck, J. T., Cole, J. E., Shanahan, T. M. and Steinitz-Kannan, M.: Holocene changes in eastern tropical Pacific climate inferred from a Galápagos lake sediment record, Quaternary Science Reviews, 27(11), 1166–1180, 10 doi:https://doi.org/10.1016/j.quascirev.2008.02.015, 2008.

Darling, K., Wade, C. M., Steward, I. A., Kroon, D., Dingle, R. and Leigh Brown, A. J.: Molecular evidence for genetic mixing of Arctic and Antarctic subpolar populations of planktonic foraminifers, Nature, 405, 43–47, 2000.

Darling, K. F., Wade, C. M., Kroon, D., Brown, A. J. L. and Bijma, J.: The Diversity and Distribution of Modern Planktic Foraminiferal Small Subunit Ribosomal RNA Genotypes and their Potential as Tracers of Present and Past Ocean 15 Circulations, Paleoceanography, 14(1), 3–12, doi:10.1029/1998PA900002, 1999.

Darling, K. F., Kucera, M., Pudsey, C. J. and Wade, C. M.: Molecular evidence links cryptic diversification in polar planktonic protists to Quaternary climate dynamics, Proceedings of the National Academy of Sciences, 101(20), 7657–7662, doi:10.1073/pnas.0402401101, 2004.

Dolman, A. M. and Laepple, T.: Sedproxy: a forward model for sediment archived climate proxies, Climate of the Past 20 Discussions, 1–31, doi:10.5194/cp-2018-13, 2018.

Du, X., Hendy, I. and Schimmelmann, A.: A 9000-year flood history for Southern California: A revised stratigraphy of varved sediments in Santa Barbara Basin, Marine Geology, 397, 29–42, doi:https://doi.org/10.1016/j.margeo.2017.11.014, 2018.

Dubois, N., Kienast, M., Normandeau, C. and Herbert, T. D.: Eastern equatorial Pacific cold tongue during the Last Glacial 25 Maximum as seen from alkenone paleothermometry, Paleoceanography, 24(4), doi:10.1029/2009PA001781, 2009.

Eggins, S. M., Sadekov, A. and de Deckker, P.: Modulation and daily banding of Mg/Ca in Orbulina universa tests by symbiont photosynthesis and respiration: a complication for seawater thermometry, Earth and Planetary Science Letters, 225, 411–419, 2003.

Elderfield, H. and Ganssen, G. M.: Past temperature and δ18O of surface ocean waters inferred from foraminiferal Mg/Ca 30 ratios, Nature, 405(6785), 442–445, 2000.

Emiliani, C.: Depth habitats of some species of pelagic foraminifera as indicated by oxygen isotope ratios, American Journal of Science, 252(3), 149–158, doi:10.2475/ajs.252.3.149, 1954.

Emiliani, C.: Pleistocene Temperatures, The Journal of Geology, 63(6), 538–578, 1955.

Enzel, Y. and Wells, S. G.: Extracting Holocene paleohydrology and paleoclimatology information from modern extreme 35 flood events: An example from southern California, Geomorphology, 19(3), 203–226, doi:https://doi.org/10.1016/S0169-555X(97)00015-9, 1997.

Ericson, D. B. and Wollin, G.: Pleistocene climates and chronology in deep-sea sediments, Science, 162, 1227–1234, 1968.

Ericson, D. B., Ewing, M. and Wollin, G.: The Pleistocene Epoch in Deep-Sea Sediments, Science, New Series, 146(3645), 723–732, 1964.

Evans, D., Müller, W. and Erez, J.: Assessing foraminifera biomineralisation models through trace element data of cultures
5   under variable seawater chemistry, Geochimica et Cosmochimica Acta, 236, 198–217, doi:10.1016/j.gca.2018.02.048, 2018.

Fallet, U., Boer, W., van Assen, C., Greaves, M. and Brummer, G. J. A.: A novel application of wet-oxidation to retrieve carbonates from large, organic-rich samples for application in climate research, Geochemistry Geophysics Geosystems, 10(8), 2009.

Feldmeijer, W., Metcalfe, B., Scussolini, P. and Arthur, K.: The effect of chemical pretreatment of sediment upon
10   foraminiferal-based proxies, Geochemistry, Geophysics, Geosystems, 14(10), 3996–4014, doi:10.1002/ggge.20233, 2013.

Feldmeijer, W., Metcalfe, B., Brummer, G. J. A. and Ganssen, G. M.: Reconstructing the depth of the permanent thermocline through the morphology and geochemistry of the deep dwelling planktonic foraminifer Globorotalia truncatulinoides, Paleoceanography, 30(1), 1–22, doi:10.1002/2014PA002687, 2015.

Ford, H. L., Ravelo, A. C. and Polissar, P. J.: Reduced El Nino-Southern Oscillation during the Last Glacial Maximum,
15   Science, 347(6219), 255–258, doi:10.1126/science.1258437, 2015.

Fraile, I., Schulz, M., Mulitza, S. and Kucera, M.: Predicting the global distribution of planktonic foraminifera using a dynamic ecosystem model, Biogeosciences, 5, 891–911, 2008.

Fraile, I., Schulz, M., Mulitza, S., Merkel, U., Prange, M. and Paul, A.: Modeling the seasonal distribution of planktonic foraminifera during the Last Glacial Maximum, Paleoceanography, 24, doi:10.1029/2008PA001686, 2009.

20   Ganssen, G. M., Peeters, F. J. C., Metcalfe, B., Anand, P., Jung, S. J. A., Kroon, D. and Brummer, G.-J. A.: Quantifying sea surface temperature ranges of the Arabian Sea for the past 20 000 years, Climate of the Past, 7(4), 1337–1349, doi:10.5194/cp-7-1337-2011, 2011.

Garidel-Thoron, T. de, Rosenthal, Y., Beaufort, L., Bard, E., Sonzogni, C. and Mix, A. C.: A multiproxy assessment of the western equatorial Pacific hydrography during the last 30 kyr, Paleoceanography, 22(3), doi:10.1029/2006PA001269, 2007.

25   Gray, W. R., Weldeab, S., Lea, D. W., Rosenthal, Y., Gruber, N., Donner, B. and Fischer, G.: The effects of temperature, salinity, and the carbonate system on Mg/Ca in Globigerinoides ruber (white): A global sediment trap calibration, Earth and Planetary Science Letters, 482, 607–620, doi:10.1016/j.epsl.2017.11.026, 2018.

Greaves, M., Barker, S., Daunt, C. and Elderfield, H.: Accuracy, standardization, and interlaboratory calibration standards for foraminiferal Mg/Ca thermometry, Geochem. Geophys. Geosyst., 6(2), Q02D13, 2005.

30   Groeneveld, J., Nürnberg, D., Tiedemann, R., Reichart, G.-J., Steph, S., Reuning, L., Crudeli, D. and Mason, P.: Foraminiferal Mg/Ca increase in the Caribbean during the Pliocene: Western Atlantic Warm Pool formation, salinity influence, or diagenetic overprint?, Geochemistry Geophysics Geosystems, 9, Q01P23, doi:doi:10.1029/2006GC001564, 2008.

Hamilton, C. P., Spero, H. J., Bijma, J. and Lea, D. W.: Geochemical investigation of gametogenic calcite addition in the
35   planktonic foraminifera Orbulina universa, Marine Micropaleontology, 68(3–4), 256–267, 2008.

Hecht, A. D.: A model for determining Pleistocene paleotemperatures from planktonic foraminiferal assemblages, Micropaleontology, 19, 68–77, 1973.

Hendy, I. L., Napier, T. J. and Schimmelmann, A.: From extreme rainfall to drought: 250 years of annually resolved sediment deposition in Santa Barbara Basin, California, Quaternary International, 387, 3–12, 5 doi:https://doi.org/10.1016/j.quaint.2015.01.026, 2015.

Higley, M. C., Conroy, J. L. and Schmitt, S.: Last Millennium Meridional Shifts in Hydroclimate in the Central Tropical Pacific, Paleoceanography and Paleoclimatology, 33(4), 354–366, doi:10.1002/2017PA003233, 2018.

Hori, M., Shirai, K., Kimoto, K., Kurasawa, A., Takagi, H., Ishida, A., Takahata, N. and Sano, Y.: Chamber formation and trace element distribution in the calcite walls of laboratory cultured planktonic foraminifera (Globigerina bulloides and 10 Globigerinoides ruber), Marine Micropaleontology, 140, 46–55, doi:10.1016/j.marmicro.2017.12.004, 2018.

Huang, B., Thorne, P. W., Banzon, V. F., Boyer, T., Chepurin, G., Lawrimore, J. H., Menne, M. J., Smith, T. M., Vose, R. S. and Zhang, H.-M.: Extended Reconstructed Sea Surface Temperature, Version 5 (ERSSTv5): Upgrades, Validations, and Intercomparisons, Journal of Climate, 30(20), 8179–8205, doi:10.1175/jcli-d-16-0836.1, 2017.

Huber, B. T., Bijma, J. and Darling, K.: Cryptic speciation in the living planktonic foraminifer Globigerinella siphonifera 15 (d'Orbigny), Paleobiology, 23(01), 33–62, doi:10.1017/S0094837300016638, 1997.

Hut, G.: Consultants group meeting on stable isotope reference samples for geochemical and hydrological investigations, Int. At. Energy Agency, Vienna., 1987.

Hutson, W. H.: Transfer functions under no-analog conditions: experiments with Indian Ocean planktonic foraminifera, Quarternary Research, 8(3), 355–367, 1977.

20 Hutson, W. H.: Applications of transfer functions to Indian Ocean planktonic foraminifera, Quarternary Research, 9, 87–112, 1978.

Hutson, W. H.: Bioturbation of deep-sea sediments: Oxygen isotopes and stratigraphic uncertainty, Geology, 8(3), 127–130, doi:10.1130/0091-7613(1980), 1980a.

Hutson, W. H.: The Agulhas Current during the Late Pleistocene-analysis of modern faunal analogs, Science, 207(4426), 25 64–66, 1980b.

Imbrie, J. and Kipp, N. G.: A new Micropaleontological method for paleoclimatology: Application to a Late Pleistocene Caribbean core, in The Late Cenozoic Glacial Ages, edited by K. K. Turekian, pp. 71–181, Yale University Press, New Haven, Connecticut., 1971.

Jacob, D. E., Wirth, R., Agbaje, O. B. A., Branson, O. and Eggins, S. M.: Planktic foraminifera form their shells via 30 metastable carbonate phases, Nature Communications, 8(1), 1265, doi:10.1038/s41467-017-00955-0, 2017.

Jones, J. I.: Distribution of living planktonic foraminifera of the West Indies and adjacent waters, PhD Thesis, University Wisconsin-Madison, Madison, Wisconsin USA., 1964.

Jonkers, L. and Kučera, M.: Quantifying the effect of seasonal and vertical habitat tracking on planktonic foraminifera proxies, Climate of the Past, 13(6), 573–586, doi:10.5194/cp-13-573-2017, 2017.

Kageyama, M., Braconnot, P., Bopp, L., Caubel, A., Foujols, M.-A., Guilyardi, E., Khodri, M., Lloyd, J., Lombard, F., Mariotti, V., Marti, O., Roy, T. and Woillez, M.-N.: Mid-Holocene and Last Glacial Maximum climate simulations with the IPSL model—part I: comparing IPSL_CM5A to IPSL_CM4, Climate Dynamics, 40(9), 2447–2468, doi:10.1007/s00382-012-1488-8, 2013.

5   Kienast, M., MacIntyre, G., Dubois, N., Higginson, S., Normandeau, C., Chazen, C. and Herbert, T. D.: Alkenone unsaturation in surface sediments from the eastern equatorial Pacific: Implications for SST reconstructions, Paleoceanography, 27(1), doi:10.1029/2011PA002254, 2012.

Kim, S.-T. and O'Neil, J. R.: Equilibrium and nonequilibrium oxygen isotope effects in synthetic carbonates, Geochimica et Cosmochimica Acta, 61(16), 3461–3475, doi:10.1016/S0016-7037(97)00169-5, 1997.

10   Kısakürek, B., Eisenhauer, A., Böhm, F., Garbe-Schönberg, D. and Erez, J.: Controls on shell Mg/Ca and Sr/Ca in cultured planktonic foraminiferan, Globigerinoides ruber (white), Earth and Planetary Science Letters, 273(3–4), 260–269, doi:10.1016/j.epsl.2008.06.026, 2008.

Koutavas, A. and Joanides, S.: El Niño–Southern Oscillation extrema in the Holocene and Last Glacial Maximum, Paleoceanography, 27(4), doi:10.1029/2012PA002378, 2012.

15   Koutavas, A. and Lynch-Stieglitz, J.: Glacial-interglacial dynamics of the eastern equatorial Pacific cold tongue-Intertropical Convergence Zone system reconstructed from oxygen isotope records: GLACIAL PACIFIC COLD TONGUE, Paleoceanography, 18(4), n/a-n/a, doi:10.1029/2003PA000894, 2003.

Koutavas, A., Lynch-Stieglitz, J., Marchitto, T. M. and Sachs, J. P.: El Niño-Like Pattern in Ice Age Tropical Pacific Sea Surface Temperature, Science, 297(5579), 226, doi:10.1126/science.1072376, 2002.

20   Koutavas, A., deMenocal, P. B., Olive, G. C. and Lynch-Stieglitz, J.: Mid-Holocene El Niño–Southern Oscillation (ENSO) attenuation revealed by individual foraminifera in eastern tropical Pacific sediments, Geology, 34(12), 993, doi:10.1130/G22810A.1, 2006.

Kretschmer, K., Kucera, M. and Schulz, M.: Modeling the distribution and seasonality of Neogloboquadrina pachyderma in the North Atlantic Ocean during Heinrich Stadial 1, Paleoceanography, 31(7), 986–1010, doi:10.1002/2015PA002819, 2016.

25   Kretschmer, K., Jonkers, L., Kucera, M. and Schulz, M.: Modeling seasonal and vertical habitats of planktonic foraminifera on a global scale, Biogeosciences Discussions, 1–37, doi:10.5194/bg-2017-429, 2017.

Leduc, G., Vidal, L., Cartapanis, O. and Bard, E.: Modes of eastern equatorial Pacific thermocline variability: Implications for ENSO dynamics over the last glacial period: ENSO DYNAMICS OVER THE LAST 50 KA, Paleoceanography, 24(3), doi:10.1029/2008PA001701, 2009.

30   LeGrande, A. N. and Schmidt, G. A.: Global gridded data set of the oxygen isotopic composition in seawater, Geophysical Research Letters, 33(12), L12604, 2006.

Lombard, F., Labeyrie, L., Michel, E., Spero, H. J. and Lea, D. W.: Modelling the temperature dependent growth rates of planktic foraminfera, Marine Micropalaeontology, 70, 1–7, 2009.

Lombard, F., da Rocha, R. E., Bijma, J. and Gattuso, J. P.: Effect of carbonate ion concentration and irradiance on
35   calcification in planktonic foraminifera, Biogeosciences, 7(1), 247–255, 2010.

Lombard, F., Labeyrie, L., Michel, E., Bopp, L., Cortijo, E., Retailleau, S., Howa, H. and Jorissen, F.: Modelling planktic foraminifer growth and distribution using an ecophysiological multi-species approach, Biogeosciences, 8(4), 853–873, doi:10.5194/bg-8-853-2011, 2011.

5 Loubere, P., Creamer, W. and Haas, J.: Evolution of the El Nino-Southern Oscillation in the late Holocene and insolation driven change in the tropical annual SST cycle, Global and Planetary Change, 100, 129–144, doi:https://doi.org/10.1016/j.gloplacha.2012.10.007, 2013.

Lougheed, B. C., Metcalfe, B., Ninnemann, U. S. and Wacker, L.: Moving beyond the age depth model paradigm in deep-sea palaeoclimate archives: dual radiocarbon and stable isotope analysis on single foraminifera, Climate of the Past, 14(4), 515–526, 2018.

10 Löwemark, L.: Importance and Usefulness of Trace fossils and Bioturbation in Paleoceanography, in Trace Fossils: Concepts, Problems, Prospects, edited by W. Miller, pp. 413–427, Elsevier, Amsterdam., 2007.

Löwemark, L. and Grootes, P. M.: Large age differences between planktic foraminifers caused by abundance variations and Zoophycos bioturbation, Paleoceanography, 19, PA2001, doi:10.1029/2003PA000949, 2004.

Löwemark, L., Hong, W.-L., Yui, T.-F. and Hung, G.-W.: A test of different factors influencing the isotopic signal of 15 planktonic foraminifera in surface sediments from the northern South China Sea, Marine Micropaleontology, 55(1–2), 49–62, doi:10.1016/j.marmicro.2005.02.004, 2005.

Löwemark, L., Konstantinou, K. I. and Steinke, S.: Bias in foraminiferal multispecies reconstructions of paleohydrographic conditions caused by foraminiferal abundance variations and bioturbational mixing: A model approach, Marine Geology, 256, 101–106, 2008.

20 Lynts, G. W. and Judd, J. B.: Late Pleistocene paleotemperatures at Tongue of the Ocean, Bahamas, Science, 171, 1143–1144, 1971.

MARGO Project Members*: Constraints on the magnitude and patterns of ocean cooling at the Last Glacial Maximum, Nature Geoscience, 2(2), 127–132, doi:10.1038/ngeo411, 2009.

McIntyre, A., Kipp, N. G., Bé, A. W. H., Crowley, T., Kellogg, T., Gardner, J. V., Prell, W. L. and Ruddiman, W. F.: Glacial 25 North Atlantic 18,000 years ago: A CLIMAP reconstruction, Geological Society of America Memoirs, 145, 43–76, 1976.

Metcalfe, B., Feldmeijer, W., de Vringer-Picon, M., Brummer, G.-J. A., Peeters, F. J. C. and Ganssen, G. M.: Late Pleistocene glacial–interglacial shell-size–isotope variability in planktonic foraminifera as a function of local hydrography, Biogeosciences, 12(15), 4781–4807, doi:10.5194/bg-12-4781-2015, 2015.

Metcalfe, B., Lougheed, B.C., Waelbroeck, C., and Roche D.M.: DATA: Data set, Zenodo, 30 https://doi.org/10.5281/zenodo.2554843, 2019

Metcalfe, B., Feldmeijer, W., and Ganssen, G.M.: Oxygen isotope variability of planktonic foraminifera provide clues to past upper ocean seasonal variability, Paleoceanography and Paleoclimatology, doi: 10.1029/2018PA003475, 2019

35 Mix, A. C.: The oxygen-isotope record of deglaciation, in: North America and adjacent oceans during the last deglaciation, in The Geology of America, vol. K-3, edited by W. F. Ruddiman and H. E. J. Wright, pp. 111–135, Geological Society of America, Boulder, Colorado., 1987.

Morard, R., Quillévéré, F., Escarguel, G., de Garidel-Thoron, T., de Vargas, C. and Kucera, M.: Ecological modeling of the temperature dependence of cryptic species of planktonic Foraminifera in the Southern Hemisphere, Palaeogeography, Palaeoclimatology, Palaeoecology, 391, 13–33, doi:10.1016/j.palaeo.2013.05.011, 2013.

Morard, R., Reinelt, M., Chiessi, C. M., Groeneveld, J. and Kucera, M.: Tracing shifts of oceanic fronts using the cryptic
5   diversity of the planktonic foraminifera *Globorotalia inflata*, Paleoceanography, 31(9), 1193–1205, doi:10.1002/2016PA002977, 2016.

Moy, C. M., Seltzer, G. O., Rodbell, D. T. and Anderson, D. M.: Variability of El Niño/Southern Oscillation activity at millennial timescales during the Holocene epoch, Nature, 420, 162, doi:10.1038/nature01194, 2002.

Mulitza, S., Wolff, T., Pätzold, J., Hale, W. and Wefer, G.: Temperature sensitivity of planktic foraminifera and its influence
10 on the oxygen isotope record, Marine Micropaleontology, 33(3–4), 223–240, doi:10.1016/S0377-8398(97)00040-6, 1998.

Nederbragt, A. J. and Thurow, J. W.: A 6000yr varve record of Holocene climate in Saanich Inlet, British Columbia, from digital sediment colour analysis of ODP Leg 169S cores, Marine Geology, 174(1), 95–110, doi:https://doi.org/10.1016/S0025-3227(00)00144-4, 2001.

Nederbragt, A. J. and Thurow, J. W.: Amplitude of ENSO cycles in the Santa Barbara basin, off California, during the past
15 15,000 years, Journal of Quaternary Science, 20, 447–456, 2006.

de Nooijer, L. J., Toyofuku, T., Oguri, K., Nomaki, H. and Kitazato, H.: Intracellular pH distribution in foraminifera determined by the fluorescent probe HPTS: Intracellular pH of foraminifera, Limnology and Oceanography: Methods, 6(11), 610–618, doi:10.4319/lom.2008.6.610, 2008.

de Nooijer, L. J., Toyofuku, T. and Kitazato, H.: Foraminifera promote calcification by elevating their intracellular pH,
20 Proceedings of the National Academy of Sciences, 106(36), 15374–15378, doi:10.1073/pnas.0904306106, 2009.

Nürnberg, D., Bijma, J. and Hemleben, C.: Assessing the reliability of magnesium in foraminiferal calcite as a proxy for water mass temperatures, Geochimica et Cosmochimica Acta, 60(5), 803–814, 1996.

Olson, P., Reynolds, E., Hinnov, L. and Goswami, A.: Variation of ocean sediment thickness with crustal age, Geochem. Geophy. Geosy., 17, 1349–1369, 2016.

25 O'Neil, J. R., Clayton, R. N. and Mayeda, T. K.: Oxygen Isotope Fractionation in Divalent Metal Carbonates, The Journal of Chemical Physics, 51(12), 5547–5558, 1969.

Parker, F. L.: Eastern Meditteranean foraminifera, Rep. Swedish Deep Sea Exped., 8(4), 219–283, 1958.

Patterson, D. T., Prokoph, A., Wright, C., Chang, A. S., Thomson, R. E. and Ware, D. M.: Holocene Solar Variability and Pelagic Fish Productivity in the NE Pacfic., Palaeontologia Electronica, 7(4), 17, 2004.

30 Peeters, F. J. C., Acheson, R., Brummer, G. J. A., de Ruijter, W. P. M., Schneider, R., Ganssen, G. M., Ufkes, E. and D., K.: Vigorous exchange between the Indian and Atlantic oceans at the end of the past five glacial periods, Nature, 430, 661–665, 2004.

Pena, L. D., Cacho, I., Ferretti, P. and Hall, M. A.: El Niño–Southern Oscillation–like variability during glacial terminations and interlatitudinal teleconnections, Paleoceanography, 23(3), doi:10.1029/2008PA001620, 2008.

Climate
of the Past

Open Access

EGU

Discussions

Peng, T.-H., Broecker, W. S. and Berger, W. H.: Rates of benthic mixing in deep-sea sediment as determined by radioactive tracers, Quaternary Res., 11, 141–149, 1979.

Phleger, F. B., Parker, F. L. and Pierson, J. F.: North Atlantic Foraminifera, Swedish Deep-Sea Expedition 1947-1948, 7, 3–9, 1953.

5 Pisias, N. G. and Mix, A. C.: Aliasing of the geologic record and the search for long-period Milankovitch cycles, Paleoceanography, 3(5), 613–619, doi:10.1029/PA003i005p00613, 1988.

Pracht, H., Metcalfe, B. and Peeters, F. J. C.: Oxygen isotope composition of final chamber of planktic foraminifera provides evidence for vertical migration and depth integrated growth, Biogeosciences Discussions, 1–32, doi:10.5194/bg-2018-146, 2018.

10 Raven, J., Caldeira, K., Elderfield, H., Hoegh-Guldberg, O., Liss, P., Riebesell, U., Shepherd, J., Turley, C. and Watson, A.: Ocean acidification due to increasing atmospheric carbon dioxide., The Royal Society,., 2005.

Reynolds, R. W. and Smith, T. M.: A high-resolution global sea surface temperature climatology, Journal of Climate, 8, 1571–1583, 1995.

Reynolds, R. W., Rayner, N. A., Smith, T. M., Stokes, D. C. and Wang, W.: An Improved In Situ and Satellite SST Analysis
15 for Climate, Journal of Climate, 15(13), 1609–1625, doi:10.1175/1520-0442(2002)015<1609:aiisas>2.0.co;2, 2002.

Rincón-Martínez, D., Steph, S., Lamy, F., Mix, A. and Tiedemann, R.: Tracking the equatorial front in the eastern equatorial Pacific Ocean by the isotopic and faunal composition of planktonic foraminifera, Marine Micropaleontology, 79(1), 24–40, doi:10.1016/j.marmicro.2011.01.001, 2011.

Rink, S., Kühl, M., Bijma, J. and Spero, H. J.: Microsensor studies of photosynthesis and respiration in the symbiotic
20 foraminifer Orbulina universa, Marine Biology, 131, 583–595, 1998.

Roche, D. M., Paillard, D., Caley, T. and Waelbroeck, C.: LGM hosing approach to Heinrich Event 1: results and perspectives from data–model integration using water isotopes, Quaternary Science Reviews, 106, 247–261, doi:10.1016/j.quascirev.2014.07.020, 2014.

Roche, D. M., Waelbroeck, C., Metcalfe, B. and Caley, T.: FAME (v1.0): a simple module to simulate the effect of
25 planktonic foraminifer species-specific habitat on their oxygen isotopic content, Geoscientific Model Development, 1–22, doi:10.5194/gmd-2017-251, 2018.

Roy, T., Lombard, F., Bopp, L. and Gehlen, M.: Projected impacts of climate change and ocean acidification on the global biogeography of planktonic Foraminifera, Biogeosciences, 12(10), 2873–2889, doi:10.5194/bg-12-2873-2015, 2015.

Ruddiman, W. F.: Pleistocene Sedimentation in the Equatorial Atlantic: Stratigraphy and Faunal Paleoclimatology,
30 Geological Society of America Bulletin, 82, 283–302, 1971.

Sadekov, A., Eggins, S. M., De Deckker, P. and Kroon, D.: Uncertainties in seawater thermometry deriving from intratest and intertest Mg/Ca variability in *Globigerinoides ruber*: UNCERTAINTIES Mg/Ca SEAWATER THERMOMETRY, Paleoceanography, 23(1), n/a-n/a, doi:10.1029/2007PA001452, 2008.

Sadekov, A., Eggins, S. M., De Deckker, P., Ninnemann, U., Kuhnt, W. and Bassinot, F.: Surface and subsurface seawater
35 temperature reconstruction using Mg/Ca microanalysis of planktonic foraminifera *Globigerinoides ruber* , *Globigerinoides*

sacculifer , and *Pulleniatina obliquiloculata*: SEAWATER TEMPERATURE RECONSTRUCTION, Paleoceanography, 24(3), doi:10.1029/2008PA001664, 2009.

Sadekov, A. Y., Ganeshram, R., Pichevin, L., Berdin, R., McClymont, E., Elderfield, H. and Tudhope, A. W.: Palaeoclimate reconstructions reveal a strong link between El Niño-Southern Oscillation and Tropical Pacific mean state, Nature Communications, 4, 2692, doi:10.1038/ncomms3692, 2013.

Schott, W.: Zur klimaschichtung der tiefseesedimente im aquatorialen atlantischen ozean, Geologische Rundschau, 40(1), 20–31, 1952.

Schott, W.: Foraminiferenfauan und stratigraphie der tiefsee-sedimente in Nordatlantischen ozean, Rep. Swedish Deep Sea Exped., 7(8), 357–469, 1966.

Skrivanek, A. and Hendy, I. L.: A 500 year climate catch: Pelagic fish scales and paleoproductivity in the Santa Barbara Basin from the Medieval Climate Anomaly to the Little Ice Age (AD 1000–1500), Quaternary International, 387, 36–45, doi:https://doi.org/10.1016/j.quaint.2015.07.044, 2015.

Spero, H. J.: SYMBIOSIS IN THE PLANKTONIC FORAMINIFER, *ORBULINA UNIVERSA* , AND THE ISOLATION OF ITS SYMBIOTIC DINOFLAGELLATE, *GYMNODINIUM BÉII* SP. NOV. [1], Journal of Phycology, 23, 307–317, doi:10.1111/j.1529-8817.1987.tb04139.x, 1987.

Spero, H. J. and DeNiro, M. J.: The influence of symbiont photosynthesis on the δ18O and δ13C values of planktonic foraminiferal shell calcite, Symbiosis, 4(1–3), 213–228, 1987.

Spero, H. J. and Lea, D. W.: Experimental determination of stable isotope variability in Globigerina bulloides: implications for paleoceanographic reconstructions, Marine Micropaleontology, 28(3–4), 231–246, doi:10.1016/0377-8398(96)00003-5, 1996.

Spero, H. J., Bijma, J., Lea, D. W. and Bemis, B. E.: Effect of seawater carbonate concentration on foraminiferal carbon and oxygen isotopes, Nature, 390(6659), 497–500, doi:10.1038/37333, 1997.

Staines-Urías, F., González-Yajimovich, O. and Beaufort, L.: Reconstruction of past climate variability and ENSO-like fluctuations in the southern Gulf of California (Alfonso Basin) since the last glacial maximum, Quaternary Research, 83(3), 488–501, doi:https://doi.org/10.1016/j.yqres.2015.03.007, 2015.

Stott, L., Poulsen, C., Lund, S. and Thunell, R.: Super ENSO and Global Climate Oscillations at Millennial Time Scales, Science, 297(5579), 222, doi:10.1126/science.1071627, 2002.

Stott, L., Cannariato, K., Thunell, R., Haug, G. H., Koutavas, A. and Lund, S.: Decline of surface temperature and salinity in the western tropical Pacific Ocean in the Holocene epoch, Nature, 431(7004), 56–59, doi:10.1038/nature02903, 2004.

Thirumalai, K., Partin, J. W., Jackson, C. S. and Quinn, T. M.: Statistical constraints on El Niño Southern Oscillation reconstructions using individual foraminifera: A sensitivity analysis, Paleoceanography, 28(3), 401–412, doi:10.1002/palo.20037, 2013.

de Vargas, C., Norris, R., Zaninetti, L., Gibb, S. W. and Pawlowski, J.: Molecular evidence of cryptic speciation in planktonic foraminifers and their relation to oceanic provinces, Proceedings of the National Academy of Sciences, 96(6), 2864–2868, doi:10.1073/pnas.96.6.2864, 1999.

de Vargas, C., Bonzon, M., Rees, N. W., Pawlowski, J. and Zaninetti, L.: A molecular approach to biodiversity and biogeography in the planktonic foraminifer Globigerinella siphonifera (d'Orbigny), Marine Micropaleontology, 45(2), 101–116, 2002.

Vetter, L., Kozdon, R., Mora, C. I., Eggins, S. M., Valley, J. W., Hönisch, B. and Spero, H. J.: Micron-scale intrashell oxygen isotope variation in cultured planktic foraminifers, Geochimica et Cosmochimica Acta, 107, 267–278, doi:10.1016/j.gca.2012.12.046, 2013.

Wang, C., Deser, C., Yu, J.-Y., DiNezio, P. and Clement, A.: El Niño and Southern Oscillation (ENSO): A Review, in Coral Reefs of the Eastern Tropical Pacific: Persistence and Loss in a Dynamic Environment, edited by P. W. Glynn, D. P. Manzello, and I. C. Enochs, pp. 85–106, Springer Netherlands, Dordrecht., 2017.

Waterson, A. M., Edgar, K. M., Schmidt, D. N. and Valdes, P. J.: Quantifying the stability of planktic foraminiferal physical niches between the Holocene and Last Glacial Maximum, Paleoceanography, doi:10.1002/2016PA002964, 2016.

White, S. M., Ravelo, A. C. and Polissar, P. J.: Dampened El Niño in the Early and Mid-Holocene Due To Insolation-Forced Warming/Deepening of the Thermocline, Geophysical Research Letters, 45(1), 316–326, doi:10.1002/2017GL075433, 2018.

Williams, D. F.: Late Quarternary fluctuations of the polar front and the subtropical convergence in the southeast Indian Ocean, Marine Micropaleontology, 1, 363–375, 1976.

Williams, D. F. and Johnson, W. C.: Diversity of Recent planktonic foraminifera in the southern Indian Ocean and Late Pleistocene paleotemperatures, Quarternary Research, 5, 237–250, 1975.

Wit, J. C., Reichart, G. J. and Ganssen, G. M.: Unmixing of stable isotope signals using single specimen δ 18O analyses, Geochemistry, Geophysics, Geosystems, 14(4), 1312–1320, doi:10.1002/ggge.20101, 2013.

Wolf-Gladrow, D. A., Bijma, J. and Zeebe, R. E.: Model simulation of the carbonate chemistry in the microenvironment of symbiont bearing foraminifera, Marine Chemistry, 64(3), 181–198, doi:10.1016/S0304-4203(98)00074-7, 1999.

Wunsch, C.: On sharp spectral lines in the climate record and the millennial peak, Paleoceanography, 15(4), 417–424, doi:10.1029/1999PA000468, 2000.

Wunsch, C. and Gunn, D. E.: A densely sampled core and climate variable aliasing, Geo-Marine Letters, 23(1), 64–71, doi:10.1007/s00367-003-0125-2, 2003.

Wycech, J. B., Kelly, D. C., Kitajima, K., Kozdon, R., Orland, I. J. and Valley, J. W.: Combined effects of gametogenic calcification and dissolution on δ18O measurements of the planktic foraminifer Trilobatus sacculifer, Geochem. Geophys. Geosyst., doi:10.1029/2018GC007908, 2018.

Žarić, S., Donner, B., Fischer, G., Mulitza, S. and Wefer, G.: Sensitivity of planktic foraminifera to sea surface temperature and export production as derived from sediment trap data, Marine Micropaleontology, 55(1–2), 75–105, doi:10.1016/j.marmicro.2005.01.002, 2005.

Žarić, S., Schulz, M. and Mulitza, S.: Global prediction of planktic foraminiferal fluxes from hydrographic and productivity data, Biogeosciences, 3(2), 187–207, doi:10.5194/bg-3-187-2006, 2006.

Zeebe, R. E. and Sanyal, A.: Comparison of two potential strategies of planktonic foraminifera for house building: Mg2+ or H+ removal?, Geochimica et Cosmochimica Acta, 66(7), 1159–1169, doi:10.1016/S0016-7037(01)00852-3, 2002.

Zeebe, R. E. and Wolf-Gladrow, D. A.: CO2 in seawater: Equilibrium, Kinetics, Isotopes, 1st ed., Elsevier, Amsterdam., 2001.

Zhang, Z., Leduc, G. and Sachs, J. P.: El Niño evolution during the Holocene revealed by a biomarker rain gauge in the Galápagos Islands, Earth and Planetary Science Letters, 404, 420–434, doi:https://doi.org/10.1016/j.epsl.2014.07.013, 2014.

5   Zhu, J., Liu, Z., Brady, E., Otto-Bliesner, B., Zhang, J., Noone, D., Tomas, R., Nusbaumer, J., Wong, T., Jahn, A. and Tabor, C.: Reduced ENSO variability at the LGM revealed by an isotope-enabled Earth system model, Geophysical Research Letters, 44(13), 6984–6992, doi:10.1002/2017GL073406, 2017a.

Zhu, Z., Feinberg, J. M., Xie, S., Bourne, M. D., Huang, C., Hu, C. and Cheng, H.: Holocene ENSO-related cyclic storms recorded by magnetic minerals in speleothems of central China, Proc Natl Acad Sci USA, 114(5), 852,
10   doi:10.1073/pnas.1610930114, 2017b.